Pharmacological unmasking of epigenetically regulated genes in renal cell carcinomas under clinical chemistry aspects

Dissertation zur Erlangung des akademischen Grades
des Doktors der Naturwissenschaften (Dr. rer. nat.)

eingereicht im Fachbereich Biologie, Chemie,
Pharmazie
der Freien Universität Berlin

vorgelegt
von

Imad Alkamal
aus Aleppo
März 2014

Die Dissertation wurde von September 2009 bis März 2014 in der Forschungsabteilung der Klinik für Urologie, Charité- Universitätsmedizin Berlin unter der Leitung von Dr. rer. nat. Hans Krause durchgeführt.

1. Gutachter: Prof. Dr. med. Dr. phil. Klaus M. Beier

2. Gutachter: Prof. Dr. rer. nat. habil. Matthias F. Melzig

Disputation am: 15.10.2014

Normal cells may bear the seeds of their own destruction in the form of cancer genes. The activities of these genes may represent the final common pathway by which many carcinogens act.

Cancer genes may not be unwanted guests but essential constituents of the cell's genetic apparatus, betraying the cell only when their structure or control is distributed by carcinogens.

John Michael Bishop 1982

[Nobel Laureate 1989]

Table of contents

Tables

Figures

Shortcuts

5-aza-CR	5-azacytidine
5-aza-CdR	5-aza-2´-deoxycytidine
AB	Antibody
AMV	Avian myeloblastosis virus
Cd	Cadmium
DNMTs	DNA methyl transferase enzymes
EFNB2	Ephrin-B2
FH	Fumarate hydratase
Hg	Mercury
HIF-α	Hypoxic-inducible factor
HMGA2	High mobility group AT-hook 2
Indels	Insertions/deletions
ING1	Inhibitor of growth family, member 1
ITGA2	Integrin alpha 2
LC	Light Cycler
MBD4	Methyl-CpG binding domain protein 4
MO-MuLV	Moloney murine leukemia virus
MT	Metallothionein
PB	Lead
PBRM1	Protein polybromo-1
qPCR	Quantitative real-time PCR
RRAD	Ras-related associated with diabetes
RCC	Renal cell carcinoma
RGE	Relative Gene Expression
RT	Room Temperature
SAGE	Serial Analysis of Gene Expression
TGM2	Transglutaminase 2
TSG	Tumor suppressor gene
TSS	Transcription start site
UPL	Universal Probe Library
VHL	Von Hippel-Lindau

1 Introduction

1.1 Cancer and modification of the genetic material

Current cancer research aims to a better understanding of this complex disease on the molecular up to the organismic level by providing new insights into:

- epidemiology
- diagnosis
- and therapy

New technological tools provided within the last 60 years after the discovery of the structure of DNA (1953) like recombinat DNA, PCR, and next generation sequencing (NGS) have tremendously accelerated the progress in understanding cancer, where cancer is now accepted as a disease of our genetic material. Cancer cells are characterized by many structural and functional changes. 400 somatically mutated cancer genes are known up to date, and can be subgrouped into deregulated “gain of function” proto-oncogenes and “loss of function” tumor suppressor genes (TSG) (Hanahan and Weinberg 2011; Stratton 2011). Current research based on the complex analyses of entire cancer genomes by NGS technologies gave insight e.g. the mutational landscape of many different tumors (Cancer Genome Atlas Research 2013; Sato, Yoshizato et al. 2013; Lawrence, Stojanov et al. 2014). In case of RCCs, Gerlinger et al. discovered a tremendous tumor heterogeneity and were able to assign specific mutations to certain points of a branched tumor-specific phylogenetic tree (Gerlinger, Rowan et al. 2012; Swanton 2012; Burrell, McGranahan et al. 2013; Gerlinger, Horswell et al. 2014). These mutation-carrying genes where further characterized as “drivers” or “passengers” depending on their position at the nexus between the trunk and the branch of the phylogenetic tree (Swanton 2012).

Among mutations that target recessive tumor suppressors and dominant oncogenes known to contribute to the carcinogenic process (tumor development) are genetic alterations (indels, chromosomal translocations, chromothripsis, fusion genes, among others) (Gerlinger, Rowan et al. 2012). More recently epigenetic changes were discovered to contribute to the carcinogenic process. These epigenetic changes (DNA methylation, histone modification, and chromosomal remodeling) are defined as heritable changes without altering the DNA sequence (Berdasco and Esteller 2010). Together these changes result in newly acquired functional changes of certain molecules (proteins) that discriminate a cancer cell from a normal cell.

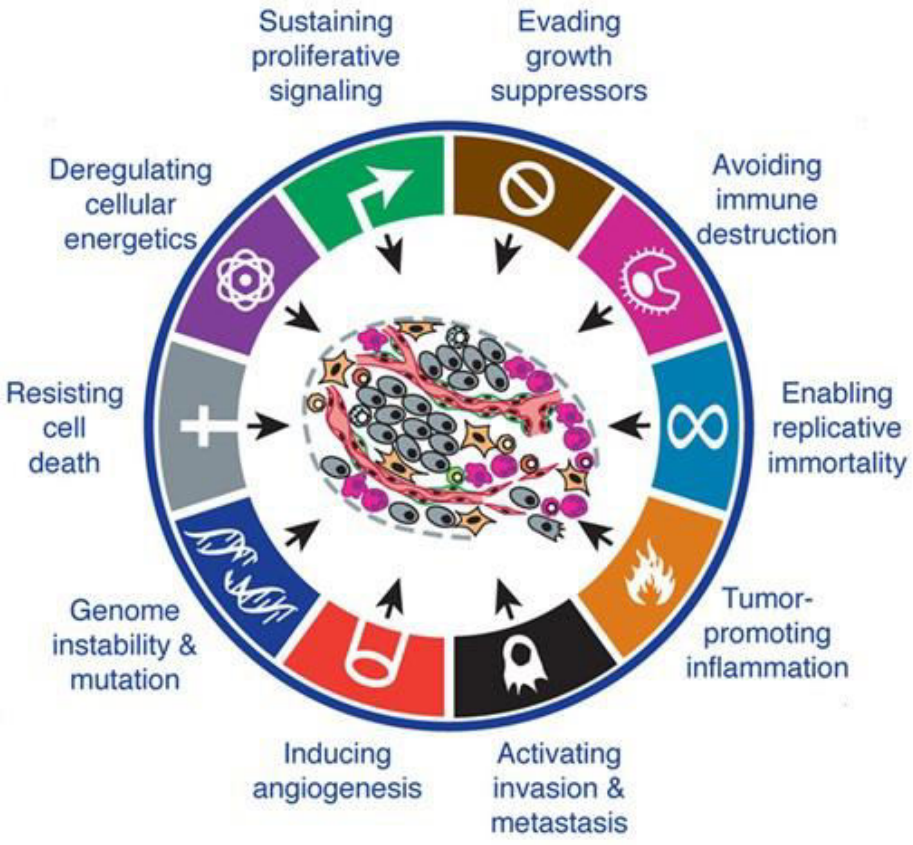

Fig. 1: Hallmarks of cancer as targets for alteration (Hanahan and Weinberg 2011)

These changes were exemplified by Hanahan & Weinberg (Fig. 1) in 2000 (extended in 2011) and include: sustaining proliferative signaling, evading growth suppressors, avoiding immune destruction, enabling replicative immortality, tumor promoting

inflammation, activating invasion and metastasis, inducing angiogenesis, genome and instability mutation, resisting cell death, and deregulating cellular energetics. Conceiving these changes, and understanding the various underlying causes would offer the opportunity for developing conceptional new therapies.

1.2 Epigenetics and gene silencing

Epigenetic deregulation as one of the underlying causes of cancer had gained great interest since the 1990s and is being studied intensively (Lee and Muller 2010). Deregulation of DNA methylation and alterations of DNA methylation patterns are described as one of the major epigenetic modifications, which contribute to various types of cancer. Epigenetic changes like global DNA hypomethylation and promoter-specific hypermethylation are observed as early events in cancer genesis. These non genetic events may also precede the “classical transforming events” like mutations in tumor suppressors, activation of protooncogenes and genomic instability (Rodriguez-Paredes and Esteller 2011).

Similiar to genetic mutations, gene-specific hypomethylation and hypermethylation of promoter regions leads to activation of oncogene transcription and/or inactivation of tumor suppressors, respectively (Scaffidi and Misteli 2010). The inactivation of a TSG by promoter methylation was first described for the retinoblastoma tumor gene (RB1) by Greger et al. in 1989 (Greger, Passarge et al. 1989).

Inactivation of TSGs by promoter hypermethylation modifies diverse cellular pathways including: cell cycle, DNA repair, toxic catabolism, cell adherence, apoptosis, angiogenesis and others (Esteller 2008). Among those TSGs targeted for transcriptional silencing and leading eventually to tumor are: APC, BRCA-1, E-cadherin, LKB1, MLH1, RB1, VHL gene in sporadic renal cell carcinoma, H19 gene in

Wilms tumors, p15 gene in leukemias, and p16INK4a in various human cancer cell lines (Esteller, Corn et al. 2001; Cheng, Matsen et al. 2003; Esteller 2008).

1.3 Mechanism of silencing tumor suppressor genes

Perceiving the mechanism of hypermethylation and gene silencing affords better means in approaching further knowledge in epigenetic research. On the nucleotide level, DNA methylation takes place in the context of CpG dinucleotides, where the C-residue is methylated at its 5-C of the pyrimidine ring. Around 30,000 CpG islands exist in the human genome and consist in general of a minimum size of 200 base pairs with a “C+G” content of more than 50% (Portela and Esteller 2010). CpG islands are located in nearly three-quarters of transcription start sites and 88% of active promoters. They regulate and render these sites as targets for potential DNA methylation and transcriptional gene silencing (Tost 2010).

Focusing on this transcriptional feature, studies have pointed out to an epigenetic cross-talk between hypermethylation and chromatin remodelling. DNA methylation as a first line of this cross-talk is mediated by DNA methyl transferase enzymes (DNMTs), whereas DNMT1 serves as the methylation maintanance and DNMT3A/B as the de novo synthesis enzymes (Kierszenbaum 2002). Together these DNMTs transfer methyl groups from S-adenosy methionine to the 5-C of cytosine residues preferentially located in promoter CpG islands and first exon of many genes (Tost 2010). Consequently, methyl-CpG binding proteins (MBDs) are recruited to those methylated promoters and interfere with binding of transcription factors to those promoters. Likewise, MBDs may recruit transcriptional correpressors like histone deacetylases (HDAC). Eventually, a compact heterochromatin structure is manifested and a transcriptional inactive chromatin environment (chromatin-repressed state) is

established leading to gene silencing (Esteller 2002; Momparler 2003; Esteller 2007; Tost 2010) (Fig. 2).

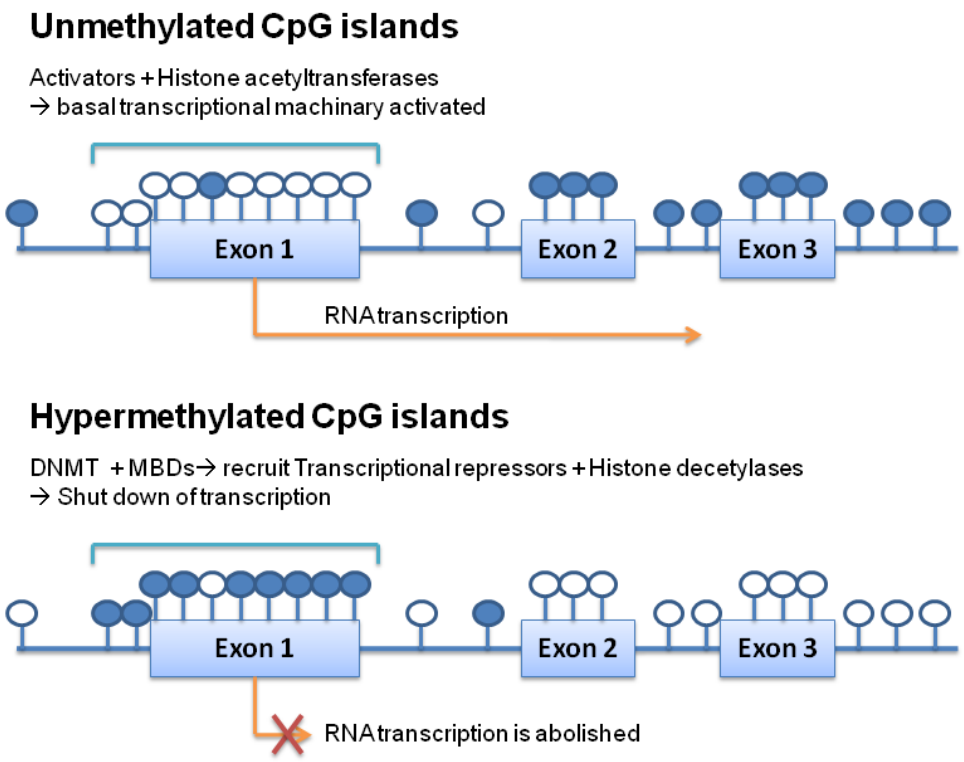

Fig. 2: CpG island in 5´region of tumor suppressor genes in normal and tumor tissues (Esteller 2002).

In contrast to genetic mutations, DNA hypermethylation is a reversible feature that can be exploited for therapeutic purposes e.g. by using DNMT inhibitors. In that sense, targeting those elements that contribute to gene silencing by reexpressing the affected genes, would render them as attractive targets for clinical treatment (Das and Singal 2004). Next to this clinical exploitation, determining genes methylated in tumors would also provide insights and offer new approaches in decoding the molecular complexity of malignancies where improved detection, diagnosis, monitoring and prognosis is always in demand (Srinivas, Verma et al. 2002).

1.4 Molecular biomarkers in cancer disease

Molecular biomarkers today comprise many different structures like proteins, nucleic acids, metabolites, and maybe assessed non-invasively in body fluids (circDNA, circulating tumor cells) or invasively in suitable tissues (Bhatt, Mathur et al. 2010; Mishra and Verma 2010).

According to their function, they may be grouped as markers for risk assessment, early diagnosis, disease stratification and prognosis, response to therapy, and monitoring of disease (Hartwell, Mankoff et al. 2006).

Since epigenetic events play important roles in cancer initiation as well as progression, current biomarker research focuses in particular on epigenetically modified structures for the discovery of reliable sensitive and cancer-specific markers.

Achieving this objective for different tumor diseases is quite promising, and kidney cancer and specifically renal cell carcinomas (RCC) are no exceptions in this concept. However, despite exhaustive research, no reliable diagnostic and prognostic biomarkers for RCC so far have been described or even used in the clinical routine (Vasudev and Banks 2011). Beside tremendous molecular insights into the pathobiology of renal cell carcinomas and the capability of certain genes to serve as molecular prognosticators (Linehan, Bratslavsky et al. 2010; Oosterwijk, Rathmell et al. 2011), pathological staging (TNM system) is still the most important prognostic indicator. Aberrant hypermethylation represents itself as an attractive target for biomarker development, since it is an early event in tumorigenesis (Laird 2003). Despite the demonstration of feasibility of methylation markers for a sensitive and specific detection of genitourinary cancers (reviewed in Carins 2007 (Cairns 2007)), the need to uncover useful new targets remains a long-standing task for the research community (Poste 2011).

1.5 Kidney cancer

1.5.1 Epidemiology and etiological factors of kidney cancer

Kidney cancer is one of the most common cancer worldwide, with an estimated 273,500 new cases diagnosed in 2008 (2% of the total). Incidence rates are lowest in Western Africa and highest in Northern America (Ferlay, Shin et al. 2010). Increased kidney cancer incidence have been reported in many different countries around the world (Mathew, Devesa et al. 2002) and it is thought to be a real increase, not only due to changes in the way the disease is diagnosed (Lynch, West et al. 2007). There is a 1.5:1 predominance of men over women, with a peak incidence occurring between 60 and 70 years of age. Etiological factors include lifestyle factors such as smoking, obesity, and hypertension (Bergstrom, Hsieh et al. 2001; Lipworth, Tarone et al. 2006; Pischon, Lahmann et al. 2006; Weikert, Boeing et al. 2008). Having a first-degree relative with kidney cancer is also associated with an increased risk of developing the disease (Clague, Lin et al. 2009). Renal cell carcinomas (RCC) represent the most common form of kidney cancers, 70-80% of the cases are classified as clear cell carcinomas (cRCC) next to papillary (pRCC, 10-15%) and chromophobe (chRCC, ~5%) subtypes. RCC has the highest mortality rate of the genitourinary cancers, as more than one third of patients will die from the disease. When diagnosed, 30% of the patients have already locally advanced or metastatic disease (Cairns 2007). Patients with metastatic disease have a median survival of 13 months, whereas the 5-year survival rate is under 10% for this group of patients (Cohen and McGovern 2005).

1.5.2 The molecular biology of kidney cancer

Renal tumorigenesis is a cellular multistep transformation process that is characterized by accumulations and interplay of genetic and epigenetic events (Arai and Kanai 2010; You and Jones 2012; Maher 2013). Seven known kidney cancer genes are involved in disorders of energy, nutrient, iron, and oxygen sensing. Therefore Linehan et al. concluded that kidney cancer is essentially a disorder of metabolism (Linehan, Srinivasan et al. 2010). Inactivating somatic and germ-line mutations of the VHL gene were among the first genetic alterations linked to RCC pathogenesis (Latif, Tory et al. 1993; Gnarra, Tory et al. 1994). Genes like MET, FLCN, FH, and SDHB are involved in the pathology of hereditary RCCs but contribute less to the development of sporadic RCCs (Morris, Maina et al. 2004). Recently, genes that are involved in epigenetic regulation of transcription (PBRM1, SETD, UTX, JARID1C) were shown to be somatically mutated to various degrees (3-41%) in sporadic RCCs (Dalgliesh, Furge et al. 2010; Varela, Tarpey et al. 2011).

Besides alterations in the DNA sequence, epigenetic alterations like histone modifications, chromatin remodelling and in particular aberrant promoter hypermethylation account for renal tumorigenesis mainly by virtue of transcriptional silencing of a multitude of genes, including known tumor suppressor genes (TSG) (Herman, Latif et al. 1994; Herman, Merlo et al. 1995). TSGs that are frequently methylated in most human cancers are infrequently methylated in RCCs (Morris, Hesson et al. 2003; Ibanez de Caceres, Dulaimi et al. 2006). Due to genome-wide scans there is a steadily increasing number of genes where CpG site/island methylation is observed in renal tumorigenesis, although the observed degree of methylation varies considerably (3-98%) (Morris and Maher 2010).

1.6 TSGs methylated in renal cell carcinoma

Tab. 1 lists candidate tumor suppressor genes associated with either one or more histological subtypes of RCC and were reported to be silenced by promoter DNA methylation.

Tab. 1: Tumor suppressor genes inactivated by DNA promoter methylation in kidney cancer

Role as tumor suppresor gene	Gene	Reference
Adhesion molecules	CASP8, CDH13 CDH1 CTNB1 LSAMP	(Chen, Lui et al. 2003; Morris, Hesson et al. 2003; Hoque, Begum et al. 2004; Costa, Henrique et al. 2007)
Apoptosis	RARB XAF1 DAPK, APAF	(Dulaimi, de Caceres et al. 2004; Christoph, Weikert et al. 2006; Lee, Huh et al. 2006)
Apoptosis signaling pathway (Wnt antagonist genes)	SFRP1, SFRP2, SFRP4, SFRP5, WIF1, DKK3	(Urakami, Shiina et al. 2006)
Cell cycle	p14ARF, p16INK4a	(Costa, Henrique et al. 2007)
DNA repair	MGMT	(Morris, Hesson et al. 2003)
Invasion/metastasis	COL1A1, TIMP3	(Dulaimi, de Caceres et al. 2004)
Detoxification gene	GSTP1	(Dulaimi, de Caceres et al. 2004)
Metabolism genes	MTHFR, ABCB1, PTGS2, FHIT, ESR1, ESR2	(Costa, Henrique et al. 2007)

Those genes are grouped according to their biological function, participating in tumorigenesis and interference in different mechanisms. VHL promoter hypermethylation, in addition to genetic LOH mutations, was reported in several studies as an additional cause for inactivating VHL expression in sporadic ccRCC (Clifford, Prowse et al. 1998). This was supported experimentally by VHL reactivation after cell line treatments with a demethylting agent (5-Aza-2´-deoxycytidine).

Methylation of promoter regions of various tumor suppressor genes that play different regulatory roles in kidney cancer have been described, too.

1.7 Reversing epigenetic demethylation and experimental reactivation of TSG

In contrast to genetic mutations, the reversibility of epigenetic modifications and in particular DNA methylation is being extensively exploited for therapeutic purposes. Therefore, reexpressed genes render them as attractive targets for clinical treatment (Das and Singal 2004). Tumor suppressor genes unmasked by reactivation treatment play various roles for example in suppressing cell growth (DNA repair, regulation of cell cycle, apoptosis, angiogenesis, metastasis), cell differentiation, and improving response to existing therapies (Cheng, Matsen et al. 2003; Yoo, Cheng et al. 2004) (Fig. 3). Exploiting the mechanisms of a “methylation-directed” gene regulation in these TSG may lead to an improved and extended understanding of tumorigenesis.

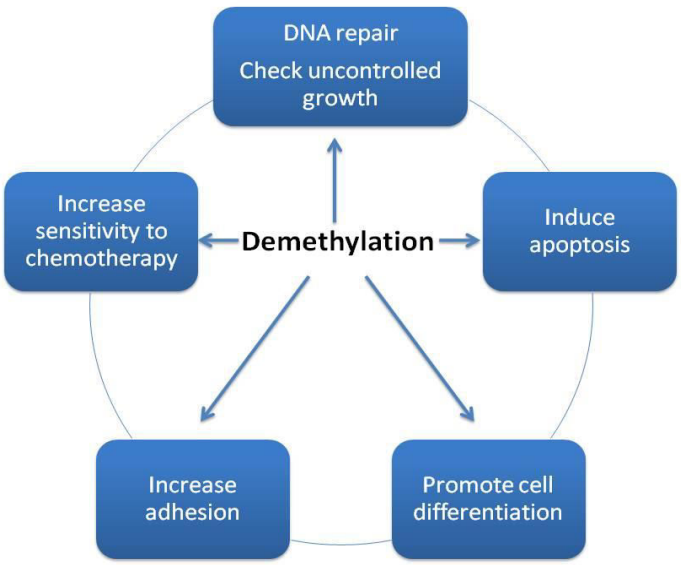

Fig. 3: Epigenetic therapy demethylates hypermethylated promoter regions of aberrantly silenced genes in tumor cells (Yoo, Cheng et al. 2004).

The so-called “epigenetic therapy”, i.e. the application of demethylating agents in cancer patients is still in its infancy (Kelly, De Carvalho et al. 2010; Mund and Lyko 2010). Some progress has been reported for hematological malignancies when DNMT inhibitors and HDAC inhibitor were used (Kelly, De Carvalho et al. 2010; Mund and Lyko 2010).

In cell line systems, global reactivation of methylated genes through inhibiting elements of transcriptional silencing (like inhibiting DNMTs) could be easily achieved by means of demethylating agents. From a historical point of view, nucleoside analogues [5-azacytidine (5-aza-CR) and its derivative 5-aza-2´-deoxycytidine (5-aza-CdR)] were developed originally as antineoplastic agents but turned out later to be powerful inhibitors of DNA methylation (Egger, Liang et al. 2004). These nucleosides incorporate to the DNA as deoxynucleotides replacing the original cytosines in the S-phase of the replicating DNA, favoring incorporation of the “fraudulent bases” into the cancer proliferating cell’s DNA (Fig. 4) (Cheng, Yoo et al. 2004). DNMT enzymes attack those new fraudulent inserted nucleosides and form a suicide complex through forming covalent bonds with their C-6 atom. The absence of an H on the N5 position prevents the resolution of the complex, leads finally to a massive loss of DNA methylation, and thus prevents further methylation of cytosine residues (Champion, Guianvarc'h et al. 2010). 5-aza-CR with a half-life of 90 minutes at 50°C in phosphate buffer saline (pH 7.4) and instability in neutral water solutions had pushed to synthesizing a more stable agent, 5-aza-CdR, but the cytotoxicity of both agents has limited their clinical administration use (Beisler 1978).

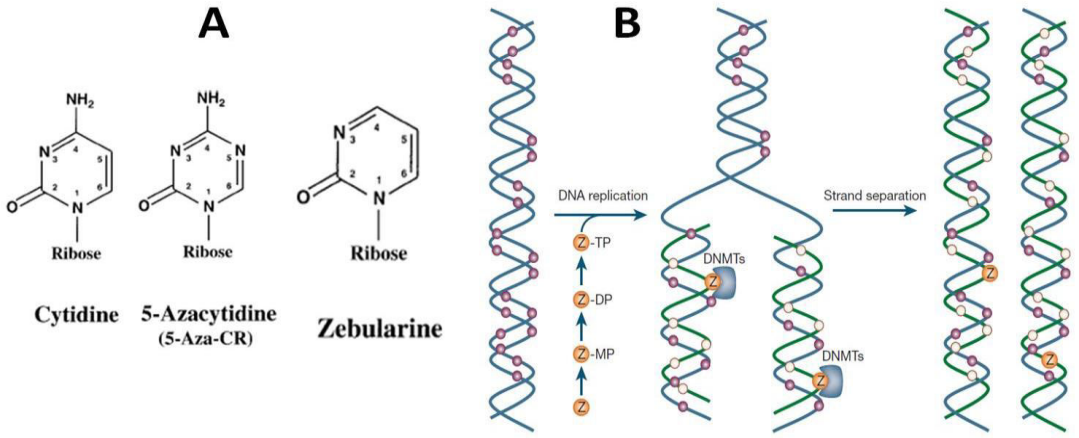

Fig. 4: A. The chemical structure for the three DNA-demethylating agents and nucleoside analogues (Cheng, Matsen et al. 2003). B. Nucleoside analogues incorporate in place of cytosines and form covalent bonds with DNMTs, depleting active enzymes and impeding methylation of DNA. Methylated CpGs: pink circles, unmethylated CpGs: white circles (Egger, Liang et al. 2004).

In comparison to the previous mentioned agents zebularine prevents the methyl group transfer by lacking the 4-amino group which usually seems to activate the cytosine C5 position for methylation (Champion, Guianvarc'h et al. 2010). It is less cytotoxic and more stable with a half-life of 44h at 37°C in PBS (pH 1.0) and around 508h at pH 7.0 which was considered to be convenient and practical for oral administration. Zebularine needs to be administrated in higher concentrations due to its function as a cytidine deaminase (which leads to its self consumption) (Yoo, Cheng et al. 2004).

Our decision to use zebularine as a DNMT inhibitor instead of the more commonly used 5-aza-CR and 5-aza-CdR goes back to initial promising experiments by Herranz et al. in 2006 (Herranz, Martin-Caballero et al. 2006). Mice exposed to radiation (radiation induced T-cell lymphoma) and treated with zebularine (400mg/kg) survived for three times longer in life than those radiation exposed control mice. In addition, a restoration of gene expression was revealed by zebularine treatment in genes including $p16^{INK4a}$, MGMT, MLT-1, and E-cadherin (Dhillon, Young et al. 2004). Moreover, demethylation was associated with the depletion of extractable DNMT1

protein by trapping of this enzyme to the zebularine-incorporated DNA. The low toxicity and acceptable antitumor activity reinforced our decision to use zebularine as a pharmacological drug for research and investigation for our experiments.

1.8 Experimental design

Experimental work took place in two phases as outlined in Fig. 5. According to our working hypothesis, demethylation of silenced genes upregulates their expression and renders them as suitable biomarker candidates. In vitro cultured A-498 cells were treated with the DNMT inhibitor zebularine. The expression of the entire transcriptome of treated and untreated cells was analyzed by RNA chip analysis. Finally a list of putative candidate genes was obtained.

In a second phase, selected candidates were validated by qPCR. A final proof of our working hypothesis would be that we could indeed reveal their diminished expression in kidney tumor tissues.

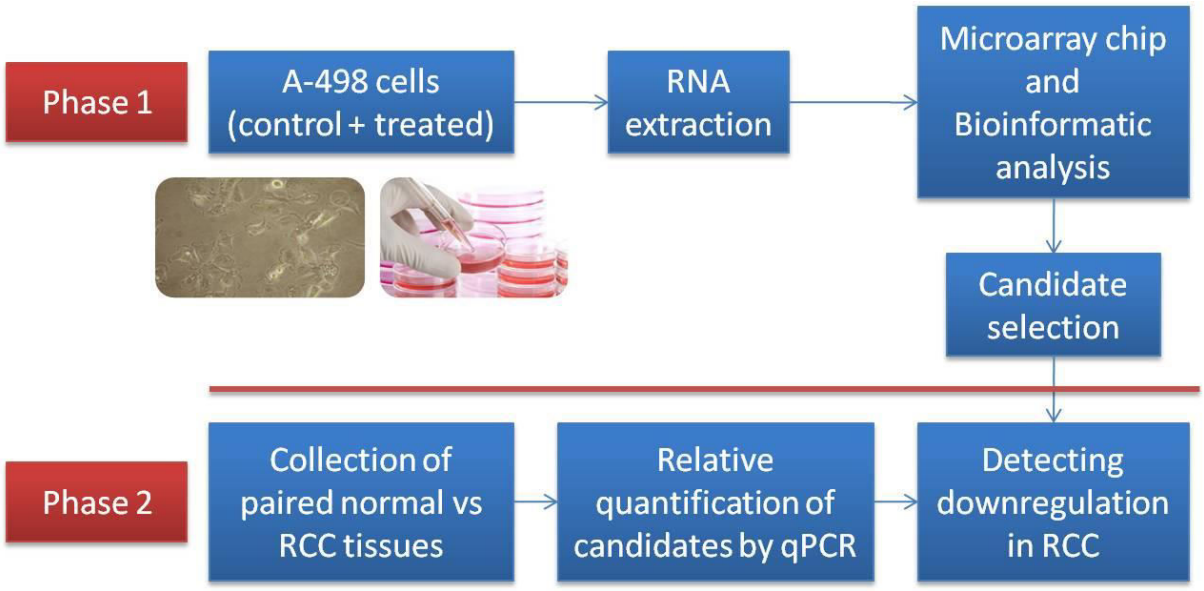

Fig. 5: Cell line reactivation of promoter hypermethylated tumor suppressor genes and investigation of candidate genes in patient renal cell carcinoma tissues.

2 Aim and objective

This study aimed to discover in RCC unkown genes that are transcriptionally silenced by promoter methylation by applying an epigenetic screen in combination with a demethylating agent.

We chose zeularine, belonging to the class of DNMT-inhibitors, as the demethylating agent based on its low cytotoxicity and its proven ability to possess measureable clinical effects.

To detect and generate a list of set of genes upregulated in A-498 cells due to zebularine treatment, we analyzed the reexpressed transcripts by means of RNA chip technology. The list of candidates was optimised by applying bioinformatic tools like CpG island prediction and SAGE analysis.

In addition to the screening results obtained from a cultured kidney tumor cell line, we evaulated the most promising candidates in clinical samples of kidney cancer patients.

In the context that no reliable biomarker for RCC is currently available, we aimed to qualify our candidates as putative epigenetically regulated biomarkers suitable for diagnosis (identification in blood, urine) and prognosis (patients chance of recovery) in kidney cancer.

3 Materials and Instruments

3.1 Materials

The following tables list the main reagents, kits, and instruments used in this work

Chapter	*Kits*	*Manufacturer*
4.1 Cell Culture		
	A-498 Cell line	*ATCC number HTB-44™ (www.atcc.org)*
	Zebularine	*SIGMA*
	RPMI 1640	Gibco (Karlsruhe, Germany)
	Dulbecco's PBS	PAA Laboratories GmbH (Pasching, Austria)
4.2 Cell proliferation andviability		
	XTT proliferation assay	Roche Diagnostics (Mannheim, Germany)
4.2.3 Western blot		
	Primary ING1 antibody (mouse)	Abcam (Cambridge, UK)
	Secondary Antibodies (antimouse)	Dakocytomation (Glostrup, Denmark)
	ECL Advance Western Blotting Detection	GE Healthcare (Buckinghamshire, UK)
	Magic Mark XP western protein standard	Invitrogen (Darmstadt, Germany)
4.3 RNA isolation & quality detection		
	RNAzol® reagent	WAK-CHMIE MEDICAL (Steinbach, Germany)
	Agilent RNA Nano kit 6000	Agilent technologies (Waldbronn, Germany)
4.4 Array Gene chip Analysis		
	Affymetrix GeneChip® Human genome U133A 2.0 Arrays	Affymetrix (Santa Clara, USA)
4.6 cDNA preparation		
	Transcriptor First	Roche Diagnostics (Mannheim,

	Strand cDNA Synthesis	Germany)
4.7 Quantitative real time –PCR		
	LightCycler480 Probes Master	Roche Diagnostics (Mannheim, Germany)
	MinElute PCR purification	Qiagen GmbH (Hilden, Germany)
	Amplification primers	TIB MOLBIOL (Berlin, Germany)
	Probes UPL	Roche Diagnostics (Mannheim, Germany)
	Quantitect SYBR Green PCR	Qiagen GmbH (Hilden, Germany)

3.2 Instruments

Chapter	*Instument*	*Manufacturer*
4.1 Cell Culture		
	Flow box	Antares
	Cell culture incubator	Binder GmbH (Tuttlingen, Germany)
	Light Microscope	Fluovert
4.2 Cell proliferation and viability		
	Multi-well spectrophotometer	Spectrophotometer Anthos htIII reader device
	Fluorescence photography	Leica DMR Fluorescence microscope
4.2.3 Western blot		
	Fluor-S Multiimager	BioRad Laboratories (Münschen, Germany)
	Xcell sureLock	Novex (San Diego, USA)
4.3 RNA isolation & quality detection		
	NanoDrop-1000 Spectrophotometer	(PeqLabs Biotechnogie)
	BioAnalyzer2100 instrument	AGILENT Technologies (Waldbronn, Germany)

4.4 Array Gene chip Analysis		Service provided by Laboratory of genome Charite/Mitte
4.6 cDNA preparation		
	Applied biosystem 9700 thermal Cycler	Applied biosystem (Foster, USA)
	Eppendorf Thermomixer 5436	Eppendorf (Hamburg, Germany)
4.7 Quantitative real time –PCR		
	LightCycler 480	Roche (Penzberg, Germany)
	Relative quantification software	GenEx (Göteborg, Sweden)
	PCR/UV work station	COY Laboratories Products (Michigan, USA)
4.7.4 **Statistical evaluation of gene expression**		
	Prism® 5	GraphPad Software
	EMBOSS-CpG blot	EMBL-EBI (Heidelberg, Germany)
	Pubmed	NCBI (Maryland, USA)

4 Experimental methods

A general outline of technologies and analytes used for the detection of genes upregulated in A-498 after treatment with the demethylating agent zebularine is given in Fig. 6.

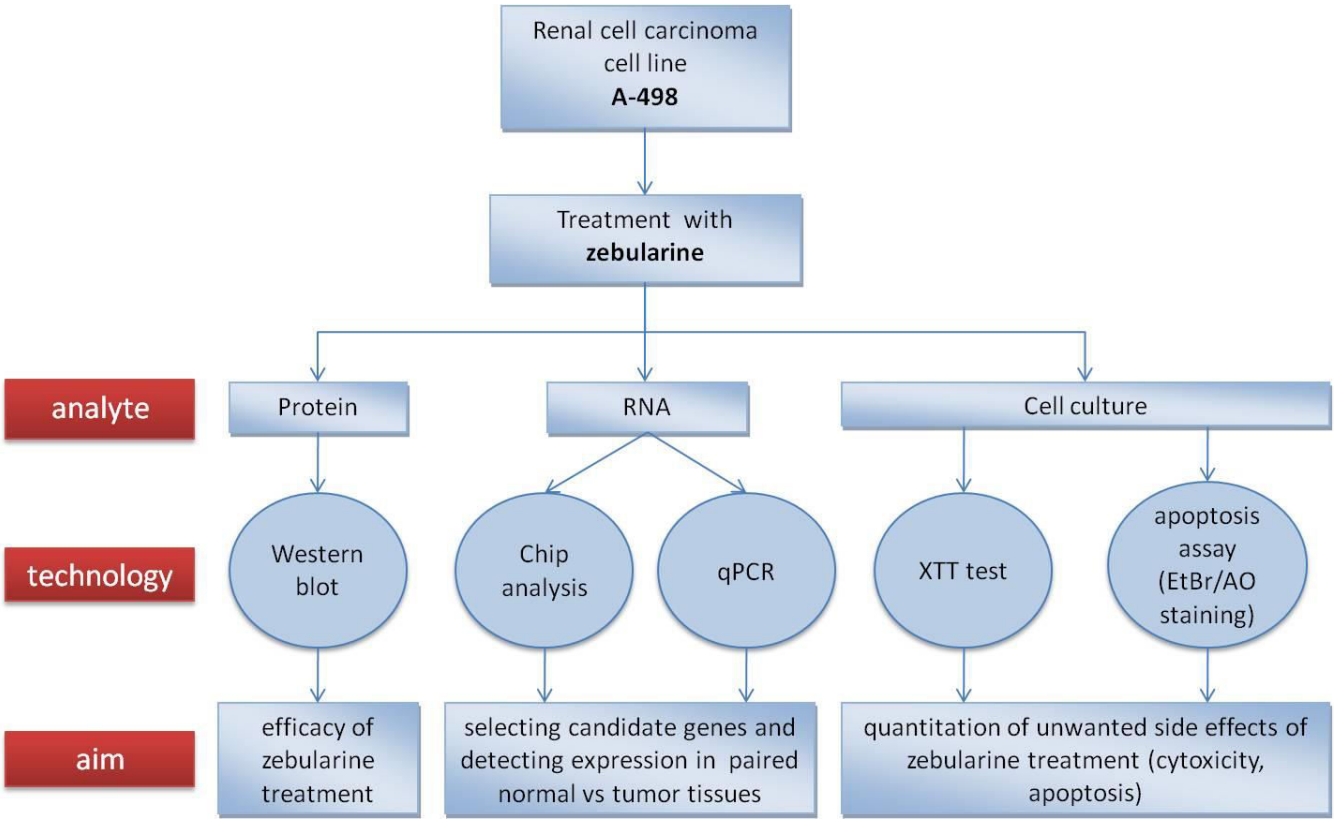

Fig. 6: Different techniques used to detect treatment efficiency on RCC cell lines (Western blot, Chip analysis, XTT test, apoptosis assay).

4.1 Cell culture and zebularine treatment

The renal cell carcinoma cell line (A-498) was cultured under sterile conditions in T75 flasks with 5mL RPMI medium supplemented with 10% FCS, 100U/mL penicillin and 100µg/mL streptomycin. Incubation took place at 37°C and 5% CO_2. For propagation, cells were detached from the surface by treatment with trypsin/EDTA solution when the cell culture reached confluence. For protein and RNA isolation, cells were

washed twice with PBS then scraped from the surface of the flask and collected by centrifugation for 5min at 1500g. The DNA methyltranserase (DNMT) inhibiting reagent zebularine was used to treat cells at final concentrations of 300µM, 500µM, and 1mM, respectively for various experimental approaches (Fig. 7). A detailed description of experiments is given in the chapters below. Treatment started usually after 24 hours of seeding. Growth medium containing zebularine was replaced after 2-3 days. Three independent treatment experiments were performed for RNA chip analysis (Fig. 7a). Cells were harvested either as cell pellets for protein extraction (Fig. 7b) or directly lysed in the culture flask for RNA isolation. In vitro cultured cells were used for viability assays (Fig. 7c-d). Cell pellets or nucleic acid preparations were kept frozen at -80ºC.

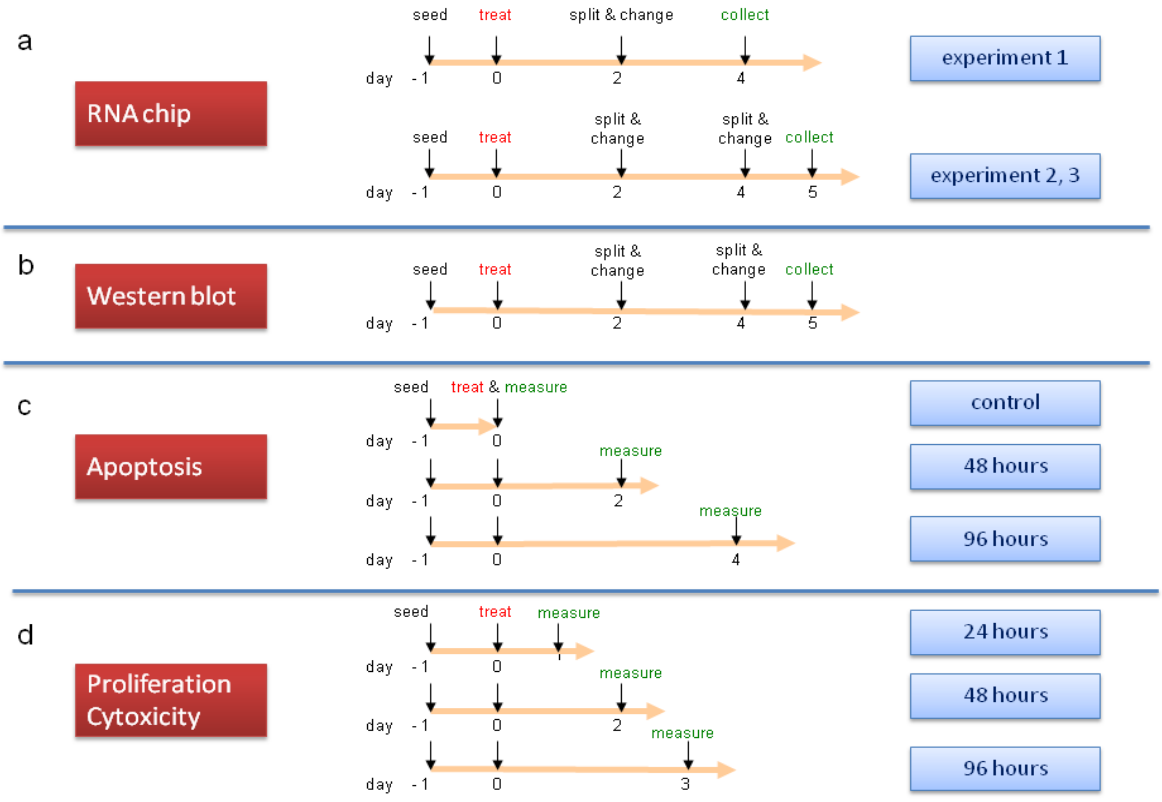

Fig. 7:Flow scheme of zebularine treatment of A-498 cells for various experimental approaches.

4.2 Cell proliferation and viability

4.2.1 Morphological assessment of apoptosis by fluorescent microscopy

A-498 cells were cultured in flasks specifically designed for microscopic analysis. Cells were treated with different concentrations of zebularine (0, 300µM, 1000µM) for definite periods of time (Fig. 7c). For morphological assessment of apoptosis by fluorescent microscopy the culture medium was exchanged with PBS containing an acridine orange/ethidium bromide mix (prepared 1:1, each 4µg/mL final concentration) and incubated for two minutes. Coverslips with attached cells were mounted and examined under fluorescent light (Leica DMR microscope). Photographs were taken at different magnifications.

Discrimination between living and dead cells was made on the base of membrane integrity. The cell membrane of a vital cell is permeable only for acridine orange allowing it to incorporate into the DNA of the cells and to stain them with a green color. Cells with damaged membranes (apoptosis and/or necrosis) are invaded by both dyes attacking the nucleus, intercalating into DNA and turning the cells into an orange color since the fluorescence of ethidium bromide (orange color) is stronger than acridine orange (green color). Determining the cell viability was carried out as the percentage of green cells (living cells) from the total number of cells seen on each chamber area.

4.2.2 XTT Proliferations-Assay

The proliferation of A-498 cells in the presence of zebularine was determined with the XTT-Test (Roche Diagnostics, Mannheim, Germany) that is based on a technology first described by Mosmann (Mosmann 1983). Vital cells are able to reduce the yellow tetrazolium salt (2,3-bis-(2-methoxy-4-nitro-5-sulfophenyl)-2H-tetrazolium-5-

carboxanilide) in the mitochondria to orange formazane. The intensity of this water-soluble dye is proportional to the number of metabolic active cells. The intensity of this dye is detected spectrophotometrically at a wave-length of 475nm.

As outlined in Fig 7d, flat-buttom 96 well plates were inoculated with A-498 cells at concentrations ranging from 1000 to 2000 cells/well. After 1 day the cells were treated with zebularine at concentrations of 300µM, 500µM, and 1000µM, repectively for a proliferation time ranging from 24 to 72 hours. At the end of each experiment XTT-Reagent (1 part activation solution : 50 parts XTT reagent) was added to the cells for four hours. Formazane dye intensity stain was measured after 4 hours at OD_{475} with the Anthos htIII multi-well spectrophotometer reader. This experiment was repeated three times and mean values were used for proliferation curves.

4.2.3 Western-Blot

Untreated and cells treated with zebularine (300µM, 500µM, 1000µM) were lysed and the protein extract was used for SDS-PAGE (12,5% w/v polyacrylamide gels). The components used for electrophoresis are given in Tab. 2.

Tab. 2: SDS-PAGE Constituents for 4 gels [according to Laemmli (Laemmli 1970)]

	Resolving Gel 12,5%T/2,6%C	**Stacking Gel 4,5% T/2,6%C**
Distilled H_2O	16.9mL	6.22mL
Resolving gel buffer (1,5 M Tris pH8,8) 36,3g Tris base ad 200mL dH_2O	10mL	-
Stacking Gel (0,5M Tris pH 6,8) 3.0 g Tris base ad 50mL dH_2O	-	2.5mL
Sodium dodecylsulfate (10% SDS) 10g SDS ad 100mL dH_2O	0.4mL	0.1mL
Monomer solution 40% Acrylamide in water (37,5:1) Serva 10681	12.5mL	1.125mL
Ammoniumperoxodisulfate (10% APS) 1.0g APS ad 10mL dH_2O	0,2mL	50µL
TEMED (SIGMA T-9281)	20µL	5µL
Volume for use	40	10

After fractionation, the protein was blotted from the SDS-PAGE gel to a PVDF-membrane by semi-dry electroblotting. The components used for semi-dry blotting are given in Tab. 3 and Tab. 4.

Tab. 3: Components of sample buffer

Solutions	Components	Volume
Sample buffer 2x concentrated, 2% SDS (Nonreduced)	- 2.5mL Stacking Gel buffer (final 0,125M) - 2.0mL glycerine (final 2%) - 2.0mL 10% SDS-solution - 100µL 1% bromophenolblue solution (final 0.01%) - ad10mL d H_2O	1mL non-reduced solution will be reduced by adding the below 20µL DTT-solution
DTT-solution	4 M DTT 0.6172g/mL	20µL
Reduced sample buffer	-980µL non-reduced sample buffer -20µL 4M DTT	20µL DTT-solution / 1mL non-reduced solution

Tab. 4: Buffers for semi-dry blotting (Western blot)

Buffer	Components	Concentration
Anode buffer I	25mM Tris base 20% methanol p.a	1.51g/500mL 100 mL/500mL
Anode buffer II	300mM Tris base 20% methanol p.a	18.15 g/500mL 100 mL/500mL
Cathode buffer	25mM Tris base 40mM 6-aminocaproic acid	1.51 g/500mL 2.62 g/500mL

Blocking of non-specific binding was made by immersing the membrane in 2% non fat dry milk in Tris-buffered saline solution containing 0,1% Tween-20 (t-TBS). This solution was also used as a washing solution between the primary and secondary antibody incubation (Tab. 5 and Tab.6).

Tab. 5: Washing solution between the two antibodies for protein detection

Washing buffer	Component	10X fold Stock solution (1:10 diluted)	1X fold final solution buffer
t-TBS (pH = 7.5)	10mM Tris base 100mM NaCl 0.1% Tween 20	12.11g 58.44g 10mL Filled up to 1L	1.211g 5.844g 1mL Filled up to 1L

Tab. 6: Sandwich composition on blotting apparatus

	Blotting reagents and materials	Blotting conditions
Upper Cathode (-ve)	6 soaked blotter paper in cathode buffer 3 soaked blotter paper in cathode buffer SDS-Gel (soaked 10min in cathode buffer) PVDF-Membrane (soaked 10 min in anode buffer I)	0,8mA/cm^2 for 1 hour
Lower Anode (+ve)	3 soaked blotting papers in anode buffer I 6 soaked blotting papers in anode buffer II	0,8mA/cm^2 for 1 hour

Afterwards the membrane was blocked with 2% non fat dry milk in t-TBS overnight at 4°C followed by incubation with the primary monoclonal antibody specific for the target protein. Horseradish peroxidase-conjugated antibody was then added as a secondary antibody. All antibody dilutions were made in 2% non fat dry milk in t-TBS solution (Tab. 7).

Tab. 7: Preparation and incubation of primary/secondary antibody

Antibody	Dilution		Incubation time at RT
Primary Antibody (anti-ING1)	1:500	1µg Ab / mL t-TBS	2 hours
Secondary Antibody	1:2500	0.52µg Ab / mL t-TBS	1 hour

This protein-antibody complex was detected through a chemi-luminescence reaction and the protein-antibody reaction was visualized by ECL Advance Western Blotting detection kit. The intensity of the detected signals by western blot was quantified with the Fluor-S Multiimager.

4.3 RNA Isolation from cultured cell lines

A-498 cells aimed for total RNA isolation were directly lysed within the flask by adding the lysis reagent RNAzolB^{TM} (Wak Chemie, Steinbach, Germany) according to the manufacturers instructions (2ml/2 x 10^6 cells). Afterwards we strictly followed the manufacturers protocol. Briefly, after a 5min incubation of the lysate at 4°C 200µL chloroform was added and then centrifuged 15min at 12000g. The upper transparent water-soluble phase was transferred to an RNase-free Eppendorf tube and RNA was precipitated by adding one volume of isopropanol. The RNA pellet was washed with 75% ethanol and dissolved in 100-200µL RNase-free water. RNA concentration and purity was determined spectrophotometrically with a Nanodrop ND-1000 instrument. All RNA samples were free from remaining proteins (260/280nm ratio ~1.8 to 2.0) and other contaminations (260/230nm ratio = 2.0 to 2.2). In addition, integrity of RNA was assessed by capillary electrophoresis on the Bioanalyzer-2100 instrument. Only samples with RIN numbers above above 9.0 were used for further analysis.

4.4 Microarray GeneChip® hybridization

Microarray GeneChip® analysis were performed at the “Labor für Funktionelle Genomforschung” (LFGC, Dr. U. Ungethüm and Dr. R.J. Kuban), a core facility of the Charité – Universitätsmedizin Berlin. Briefly, mRNAs of untreated and zebularine-treated cells of three independent biological experiments (chapter 4.1) were assessed for expression levels using Affymetrix Human Genome U133A 2.0 GeneChip® which contains approximately 22.000 probes representing 14.500 human genes. After hybridization of the corresponding cDNAs, six microarrays were analyzed using the Affymetrix Gene Chip Scanner 3000. GeneSpring software and additional open-source software were used for further bioinformatic processing by

which data files were generated and offered by the same above mentioned core facility. A brief outline of the chip analysis experiment is depicted below (Fig. 8).

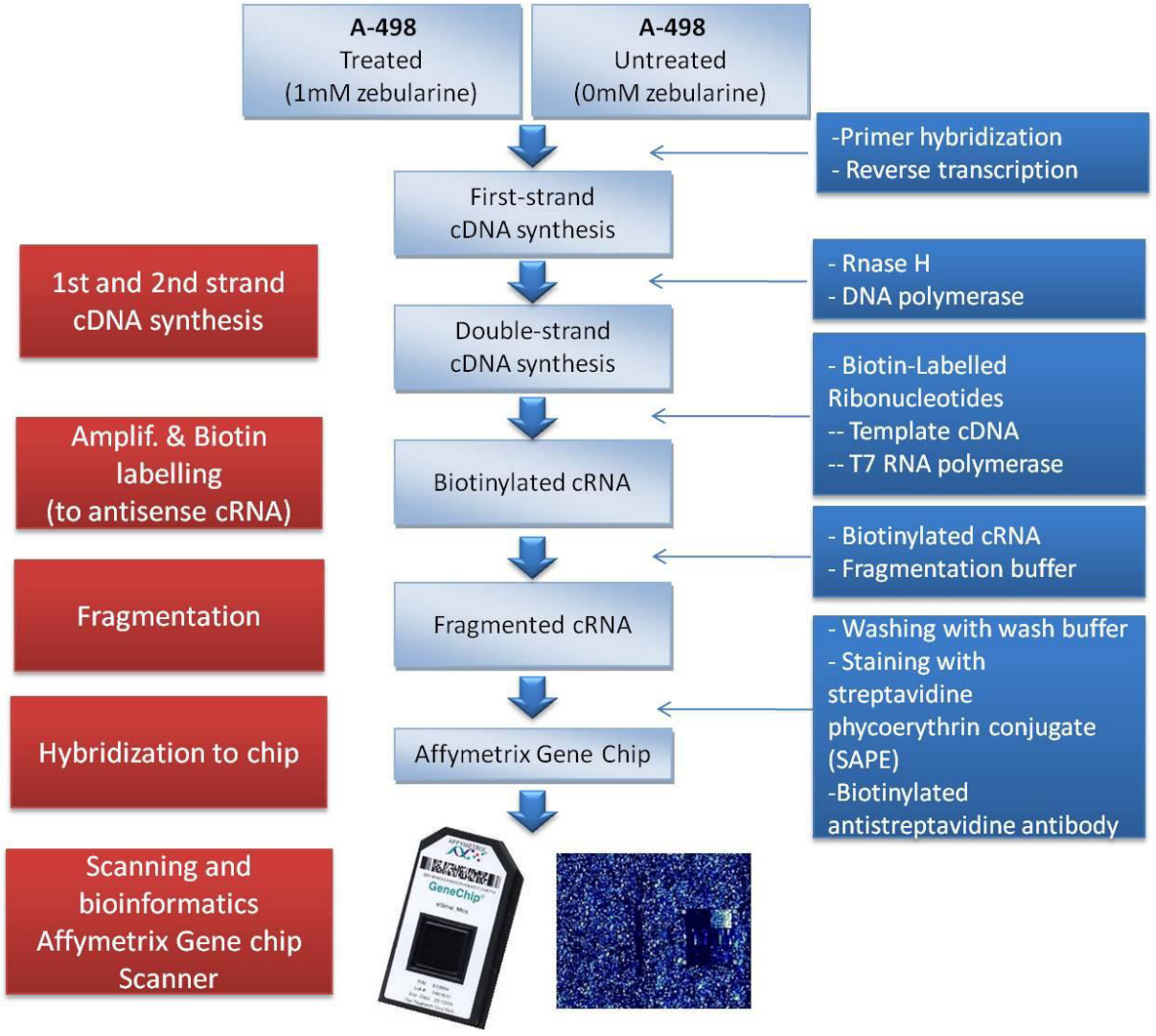

Fig. 8: Flow schema for the Affymetrix microarray gene chip hybridization

4.5 Human kidney tissue asservation and RNA preparation

In collaboration with a team of clinicians of the Department of Urology and pathologists of the Institute of Pathology, Charité – Universitätsmedizin Berlin we collected normal and tumor kidney tissue obtained after radical nephrectomy from 49 patients who underwent surgical treatment between May 2009 and October 2010. All patients gave their informed consent for this procedure in accordance with

regulations by the local ethics committee and signed a contract for anonymous material transfer for research purposes ("Stationärer Behandlungvertrag").

Briefly, after laparoscopic or open radical nephrectomy tumor-bearing kidneys were removed and perfused with cold saline buffer for approximately 20min by the laboratory team to remove blood that would interfere with subsequent molecular analysis. Under supervision of an experienced pathologist approx. 5 x 5 x 5mm cubes of normal and tumorous tissue were obtained from the respective kidneys. Paired specimens were immediately snap-frozen in liquid nitrogen and later stored at -80°C for nucleic acid isolations. Clinical data, and histopathological data (grade, stage. etc.) were obtained for each individual case and stored anonymously in a local FileMaker® database on a secured server. For nucleic acid isolation frozen tissue blocks were mounted at -25°C in a "Jung Frigo-cut 2800E" instrument and serially sectioned. These slices were immediately lysed with RNAzolB^{TM} reagent. Further handling of the samples followed the procedures described in chapter 4.3. Total RNA was dissolved in 100 – 200µL 10mM Tris-HCl, pH 8.0. Concentration was measured with a Nanodrop-1000 spectrophotometer instrument. Integrity of RNA was assessed by capillary electrophoresis using the Bioanalyzer-2100 instrument. Only samples with RIN numbers above 7.0 were used for further analysis.

4.6 cDNA synthesis

For quantifying the mRNA expression of candidate genes, 1µg total RNA was reverse transcribed into 20µL cDNA template using the reagents of the "Transcriptor First-Strand cDNA Synthesis Kit" according to the manufacturer's instructions.

Briefly, random hexamer primers were used and incubation was performed at 25°C for 10min followed by 30min incubation at 55°C. Inactivation of the reaction took

place at 85°C for 5min. Usually 1/10th to 1/20th of cDNA was subsequently used for PCR amplification (Tab. 8).

Tab. 8: Components of 13µL RNA/ primer mixture and 7µL cDNA synthesis mix for cDNA synthesis

RNA/primer mixture	**Volume (13µL)**
Total RNA	Variable (1µg)
Random hexamer primers	2µL (50µM)
DEPC-treated water	Variable (up to 13µL)
cDNA synthesis mix	**Volume (7µL)**
Transcriptor Reverse transcriptase reaction buffer	4µL
Protector RNase Inhibitor	0.5µL
Deoxynucleotide Mix (10mM)	2µL
Transcriptor Reverse Transcriptase	0.5µL

4.7 Quantitative real time-PCR

4.7.1 General introduction into qPCR and relative Gene expression (RGE)

Contrary to so-called “endpoint” detections systems (e.g. standard block cyclers) qPCR instruments detect the amplification of the target during every PCR cycle. This is done either by using unspecific incorporation of DNA intercalating fluorescent dyes like SYBR Green into the amplicon, or by probe based detections that use hybridization of gene-specific probes to the amplicon. The latter detection systems attach specific fluorescent dyes to the probes that hybridize to the amplicon. The principal advantage of these probe-based systems (using either “hybridization probes” or “hydrolysis probes”) lies within its improved specificity for the specific target sequence. In all systems, accumulation of the amplicon is detected when fluorescent signals first rise above a threshold that is around 10 times the standard deviation of the fluorescent value of the baseline. The threshold value (C_t) is the cycle number by which the fluorescence crosses the threshold. This C_t value is inversely proportional to the concentration (amount) of initial template (starting

template). The higher the initial template concentration, the faster the threshold is crossed and the lower the C_t value is obtained.

Since Taq polymerase only amplifies DNA, mRNAs have first to be converted into cDNA by a reverse transcription step (using AMV- or Mo-MuLV reverse transcriptase, or a mixture of both, see chapter 4.6). These two steps (reverse transcription and PCR amplification) may be carried out separately (two-step reaction) or in a one-step reaction, were cDNA synthesis and PCR amplification is performed in a single tube containing both enzymes - reverse transcriptase and a heat-stable DNA polymerase. Choosing the appropriate method depends upon the foreseen purpose since each of both methods (one and two steps) has its own advantages and limitations.

“Relative gene expression” (RGE) assessment is carried out to compare the expression of a particular gene of interest between samples “relative to each other” in order to determine the fold up- or downregulation of that gene. A normalization process using one or more reference genes is mandatory to ensure a reliable comparison of RGE data (i.e. exclusion of differences in quality and/or quantity of input material). Suitable reference genes which themself are not regulated will be co-amplified together with the target gene(s).

For gene expression calculation by qPCR two principal methods exist:

1. The “Comparative C_t Method” ($\Delta\Delta C_t$), a more basic approach that requires no standard curves. A prerequisite for applying this method for RGE calculation is that PCR efficiencies for target and reference genes should be close to the theoretical maximum of 2, i.e. a duplication of amplicon number during each cycle.
2. The “Relative standard curve method”, is seen as a more advanced method for calculation of RGE data (mandatory in cases where PCR efficiency differs). Such an approach requires the generation of standard curves for each

candidate and reference gene and is considered to give the most accurate quantitative results since each C_t value from unknown samples are interpolated with the standard curve and normalized to its efficiency (E).

Standard curves are generated by serial dilution of appropriate templates (RNA, PCR-fragments), stored as external files, and linked to the (automatic) RGE calculation process by including known standards into each run.

We used the $\Delta\Delta C_t$ method for validating our microarray expression data (chapter 4.7.3) and the relative standard curve method for the evaluation of our candidate genes. An inter-run calibrator (usually a known positive sample) is also included that serves to normalize for differences between different runs.

Relative gene expression (RGE = ratio target/reference) is a ratio based on the expression of target to reference gene between normal and tumor tissues and is calculated according to the following equation:

Relative expression: $E_{target}^{\Delta Ct_{target}(control - sample)} / E_{reference}^{\Delta Ct_{ref}(control - sample)}$

This RGE value is by definition dimensionless and compares gene expression in paired tissues.

4.7.2 Applying UPL qPCR technology

“Universal Probe Library” technology (UPL) is a trade mark of Roche Diagnostics GmbH. It is based on a simplified and streamlined qPCR protocol that uses web-based probe and amplification primer selection. Approximately 7000 transcripts of the human transcriptome will be detected by one singular UPL probe (out of 165 available). This high transcript coverage for UPL probes is due to their short length (8-9 nucleotides) that offer higher sequence binding possibilities in comparison to the standard Taqman probes. The amplification primers designed for the specific target

sequence bring in specificity for a particular amplicon. To maintain the hybridizing conditions for UPL probes, an enhanced type of DNA nucleotide analogues called “Locked Nucleic Acids” or “LNA”, which are nucleotides with locked ribose conformations (containing a methylene bridge between 2´-O atom and 4´-C atom) are incorporated into the UPL probes enhancing their thermal stability and binding strengths.

Amplification primers for candidate genes and probes for the reference gene PBGD were purchased from TIB MOLBIOL Berlin (Table 8 and 9). UPL probes for candidate genes were purchased from Roche Diagnostics GmbH (Tab. 9 and Tab. 10). Components of the amplification reaction mix and the block cycler conditions for synthesizing Amplicons/PCR products are listed in Tab. 11 and Tab. 12.

Tab. 9: Primers and probes for target genes obtained from Roche (UPL) to detect gene expression

Accession no.	Gene and sequence (5’->3’)	UPL Probe no.	Amplicon (nt)
	EFNB2		
NM_004093	F_TCTTTGGAGGGCCTGGAT R_CCAGCAGAACTTGCATCTTG	79	95
	ITGA2		
NM_002203	F_TCGTGCACAGTTTTGAAGATG R_TGGAACACTTCCTGTTGTTACC	7	71
	RRAD		
NM_001128850	F_AGCGTTTACAAGGTGCTGCT R_CAATGGAGCGATCATAGGTG	34	127
	MT2A		
NM_005953	F_CTTCAGCTCGCCATGGAT´ R_TGCATTTGCACTCTTTGCAT	68	91
	MT1H		
NM_005951	F_TGGGAACTCCAGTCTCACCT R_CATTTGCACTTTTTGCACTTG	68	106
	MT1G		
NM_005950	F_CCTTCTCGCTTGGGAACTCT R_CaGGTGCAGGAGACACCA	68	83
	TGM2		
NM_004613	F_ GGCACCAAGTACCTGCTCA R_ AGAGGATGCAAAGAGGAACG	1	70
	MBD4		
NM_003925	F_ GGCAACGACTCTTACCGAAT R_ CCCAAAGCCAGTCATGATATTT	38	94

Tab. 10: Primers for reference gene PBGD obtained from TIBmolbiol used for calculating the relative gene expression (RGE)

Accession no.	PBGD	Sequence (5'->3')	Amplicon (nt)
NM_000190	Primers	F_GGC TGCAACGGCGGAA R_CCTGTGGTGGACATAGCAATGATT	92
	Probe	6FAM-CGGACAGTGTGGTGGCAACATTGAAA-BBQ	N/A

Tab. 11: Components of the amplification reaction mix for generating PCR-products

Reagents	Volume [µL]	Final concentration
Template cDNA	1	10-50ng/20µL
Buffer (x10)	2	-
$MgCl_2$ (25mM)	1.6	2mM
dNTPs (2,5mM)	1.6	0.2mM
Upstream-Primer (10µM)	0.4	0.2µM
Downstream-Primer (10µM)	0.4	0.2µM
Enzyme	0.2	-
ddH_2O	12.8	-
Total volume	20	

Tab. 12: Running conditions of Block-Cycler device for gene amplification

Program	Conditions	
	Temperature	Time duration [min]
Pre-incubation	94°C	15:00
Amplification (35 cycles)	94°C	00:30
	59°C	00:30
	72°C	00:30
Extension time	72°C	07:00
Cooling	4°C	Continuously

4.7.3 Generating standard curves, measuring tissue samples and evaluations

Fig. 9 summarizes the technical steps used for assessing cell line treatment and determining RGE for each candidate gene.

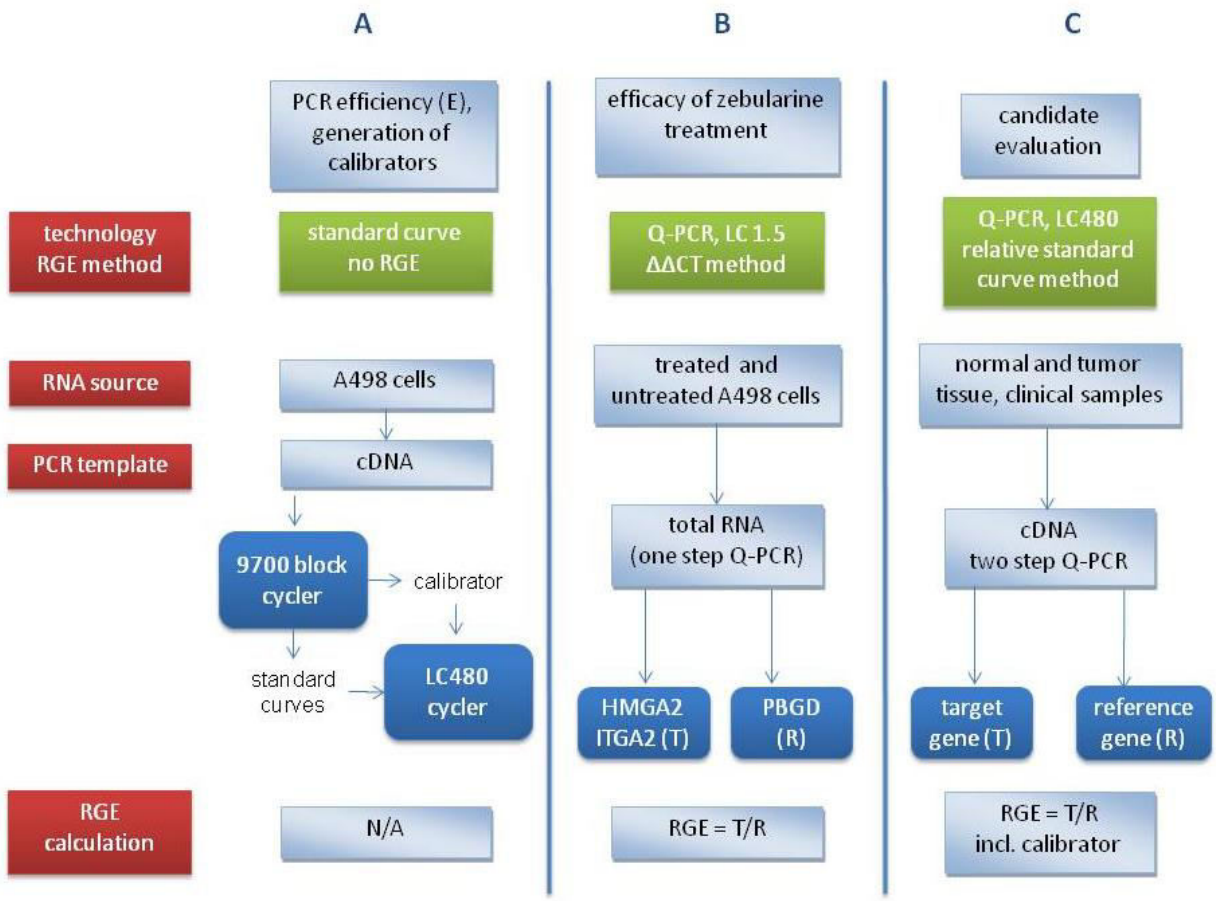

Fig. 9: Flow scheme for the different steps used for carrying out final RGE calculations: A) Generating calibrators and standard curves: used as a prerequisite for calculating the amplification efficiency (E) for later determinations of RGE [for C]. B) $\Delta\Delta C_T$ method: RGE determination using an already known Efficiency (around 2) and independent from any standard curves. C) Determining the RGE using calibrator and standard curve for corresponding candidate genes from both normal and tumor tissue samples

For the generation of standard curves Fig. 9 (A), amplicons were synthesized on a 9700 ABI instrument from cDNAs reverse transcribed from A-498 cells. PCR products were column-purified (MinElute Kit, QIAGEN) and used in 1:10 serial dilutions for at least five subsequent dilution steps. Amplification curves were generated on the LC480 instrument from duplicate, triplicate, and quadruplicate reactions for each data point. Integrated software allowed for PCR efficiency estimation that was in the range of 1.85 to 2.00. Mono-color FAM labeled Taqman probes emitting fluorescence signals at wave length of 483-533nm were used in the

reaction mix (Tab. 13) for each individual candidate gene and real time qPCR was carried out in 45 cycles by LightCycler 480 (Tab. 14). Standard curves were generated out of these points and acceptable slope/efficiency values for all candidate/reference genes were determined for later normalizaton.

Patient RNA samples from both normal/tumor tissues were reversed transcribed into cDNA (chapter 4.6) and applied in 10µL reactions to 96 wells as triplicates to calculate the mean average and to deselect values that are outliers. Duplicates of Master mix samples lacking any template (no template controls, NTC) were included in each run as a blank to detect foreign contaminations that may interfere with amplification (false positives). Internal calibrators and standards were included in each run for result normalization and evaluation (chapter 4.7.1).

Tab. 13: Components for the reaction mix from Roche (LightCycler480 Probes Master kit)

Reagents	Volume [µL]
H_20	3.4
Upstream-Primer (10µM)	0.25
Downstream-Primer (10µM)	0.25
Probe (Universal Probe Library)	1
Master Mix	5
cDNA template	1
Total volume	10

Tab. 14: Running conditions of LC480 for gene amplification

Program	Temperature	Hold	Cycles
Pre-incubation	95°C	10:00 min	1
Amplification	95°C	00:10 sec	45
	59°C	00:20 sec	
	72°C*)	00:01 sec	
Cooling	40°C	00:30 sec	1

*) Fluorescence measurements for Mono-color FAM labeled Taqman probes took place at the end of each cycle at a wave length of 483-533nm.

4.7.4 Statistical evaluation of gene expression

Statistical evaluations for normal vs. tumor gene expression (with corresponding graphs) and corelation of MTs expression with clinicopathological data were carried out by Prism® 5 software. Differences in gene expression between normal and tumor tissues from the same patient were analyzed using the paired t-test which compares the difference between set of pairs. A P-value below 0.05 was considered to be significant.

MTs expression of tumor tissues was correlated to clinicopathological data using the Spearman nonparametric correlation test. The correlation coefficient (r) ranges from -1 to +1. A value of 1 indicates a perfect correlation between two variables, a value between 0 to 1 indicates a tendency for both to increase or decrease together, a value of 0 indicates no variation between them at all, a value of 0 to -1 indicates that one variable increases as the other decreases, and a value of -1 indicates a perfect negative or inverse correlation.

4.8 Bioinformatic analysis

The following preanalytical bioinformatic analysis were applied to deliver an optimised candidate list for further evaluation:

- CpG island detection
- Serial Analysis of Gene Expression – (SAGE)

4.8.1 CpG island detection

The presence of one or multiple CpG islands in the promoter region of a particular gene is thought to be a strong indicator for a possible downregulation by promoter

hypermethylation. Computer-aided CpG island prediction is a useful tool to assess the presence of CpG islands in gene promoters.

Briefly, the promoter sequence of the gene in question was obtained from the NCBI website (http://www.ncbi.nlm.nih.gov/gene, GRCh37.p5 Primary Assembly, GenBank file format) and was analyzed online by the EMBOSS CpGPlot software provided by the EMBL-EBI website (http://www.ebi.ac.uk/Tools/emboss/cpgplot/). To cover the entire promoter we extended the sequence by adding 5000nt to the 5' end of the published sequence. For CpG island prediction we used the standard settings provided by CpG plot software. CpG islands were plotted as bars along their position preferably around the TSS within the promoter region. Typical results are depicted in Figs 14, and 17, respectively.

4.8.2 Serial Analysis of Gene Expression – (SAGE) Anatomic Viewer

In addition to CpG island prediction we wanted to know about the general expression status of our candidate genes in human kidney tissue(s). We reasoned that suitable candidates should display a higher expression in normal tissue when compared to tumorous tissue. We chose the "SAGE anatomic viewer" (SAGE Genie website, http://cgap.nci.nih.gov/SAGE/) that eases viewing expression of various transcript levels of any gene between normal and malignant tissues of a human body. Expression levels are color coded according to the color schema of the SAGE Anatomic Viewer (Boon, Osorio et al. 2002).

Based on a short 9-10bp nucleotide sequence tag (defining a certain transcript), expression levels are differentiated between tissues with a red color indicating the highest expression, and a dark blue color defining the lowest expression of a certain transcript.

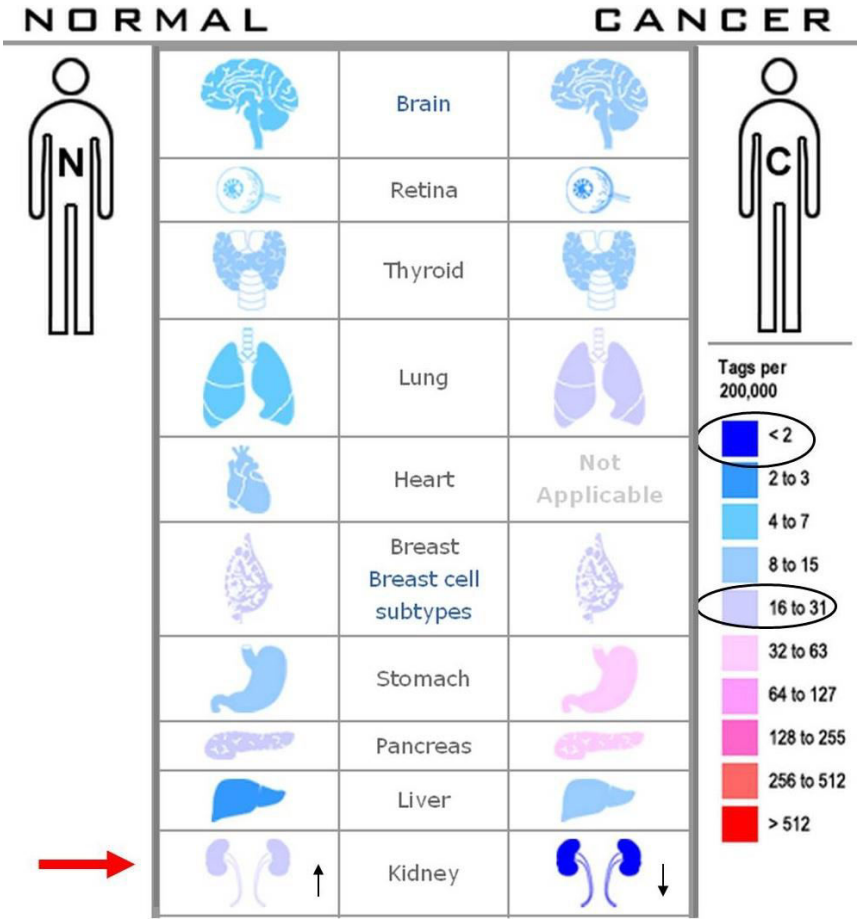

Fig. 10: SAGE anatomic viewer: Expression profile for the CLK1 gene showing an upregulation in normal kidney tissue over the malignant tissue

Fig. 10 shows an example with regard to CLK-1 gene expression between normal and malignant tissue. The normal kidney tissue appears with an average expression of 16-31 tags per 200.000 compared to malignant kidney tissue with an average expression of less than 2 tags per 200.000, indicating the elevated expression of CLK-1 in normal tissue. Genes displaying a similar expression pattern can be regarded as good suspects for further analysis of human tissue specimens by qPCR (chapter 4.7).

5 Results

5.1 A-498 cell line for discovery of transcriptionally silenced genes in RCC

In our experiments A-498 cells served as an invitro model for RCC. This ATCC cell line (ATCC® HTB-44™) was derived from a kidney carcinoma of a 52 year old female patient and is a p53 wild type. Since no data on zebularine toxicity were available for this cell line we applied several tests to determine optimal conditions for effective treatment as outlined below.

5.1.1 A-498 cell proliferation

In a first experiment, A-498 cells were treated for 5 days with different concentrations of zebularine to evaluate any antiproliferatve/cytotoxic effect of the compound. The morphology of the cells was detected photographically (Fig. 11). At day one and day five after treatment, zebularine showed no damaging effects (e.g. rounding or massive detachments) on the three used concentrations (300µM, 500µM, 1000µM) referring to zebularine's low cytotoxicity and allowing the use of 1000µM to treat A-498 cell line.

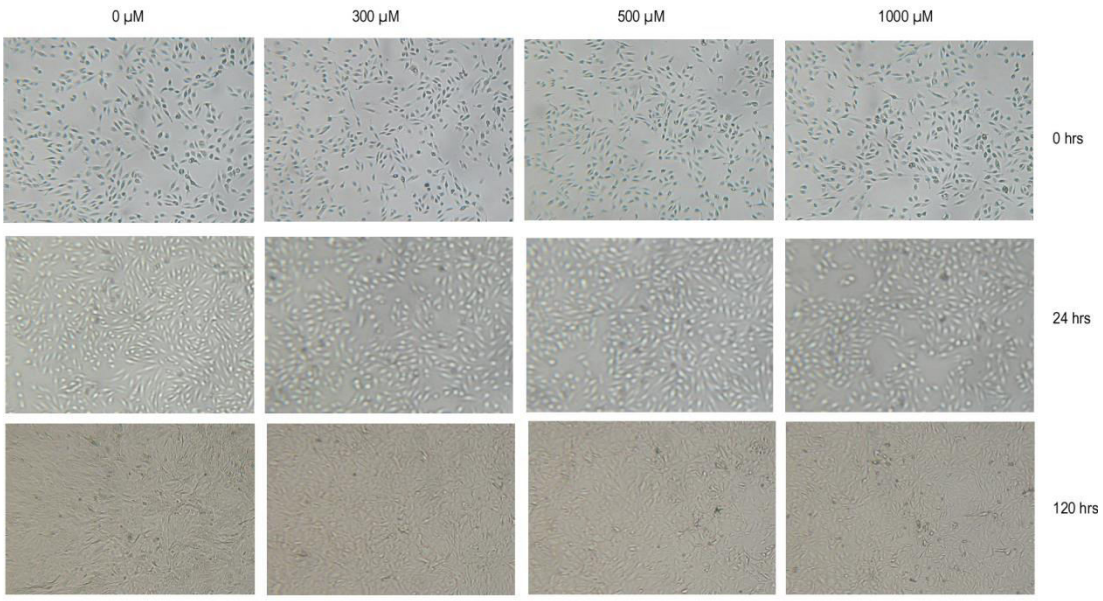

Fig. 11: Microscopic observation of A-498 cells growth after treatment with different concentrations of zebularine. Cells were exposed to four concentrations (0, 300µM, 500µM, 1000µM) and observed for growth behavior at starting point, one day after treatment and five days of treatment

5.1.2 Acridine orange/ethidium bromide assay

A second experiment with regard to antiproliferative/cytotoxic effect was made to detect specifically the necrotic and/or apoptotic influence of zebularine on the A-498 cells (as described in materials and methods). The combined uptake of an equimoloar mixture of acridine orange and ethidium bromide by A-498 cells was documented by fluorescence photography. Damage to the integrity of the cell membrane serves as a distinctive criterion between intact or apoptotic/necrotic cells. As shown in Fig. 12 less than 20% of the cells were irreversibly damaged due to zebularine treatment and no inhibitory effect on cell growth for both concentrations (300µM, 1000µM) could be detected after 48h and 96h. The latter observation was confirmed by the XTT test (Fig. 13).

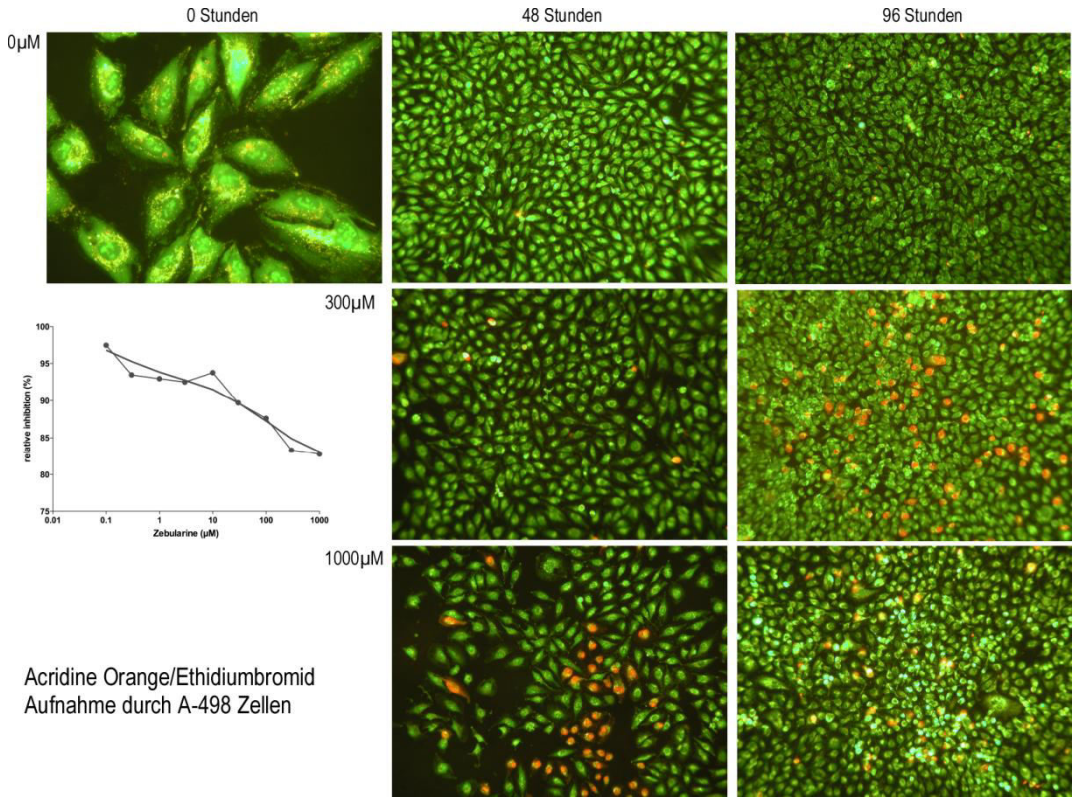

Fig. 12: Fluorescence photography for cell uptake of Acridine Orange/Ethidium bromide substances. Detection of membrane integrity for cells treated with zebularine (300µM, 1000µM) for the starting point, after two and after four days in comparison with the control cells

5.1.3 XTT proliferation test

To evaluate the influence of zebularine on A-498 proliferation in a quantitative manner, the colorimetric XTT test was carried out in a 96 well plate format. 1000-2000 cells per well were treated with different concentrations of zebularine (0 - 1000µM) and incubated for 5 days (120 hours). The XTT test was carried out according to the manufacturer instructions (chapter 4.2.2) and evaluated by a multiwell spectrophotometer reader. Data are presented as % inhibition of cell proliferation. The aim of this experiment was to detect the highest effective concentration of zebularine while cells are still proliferating and able to incorporate the modified nucleotide. As can be seen from Fig. 13, a tolerable inhibition of proliferation was measured between 60-90% for 1000-2000 cells/well respectively.

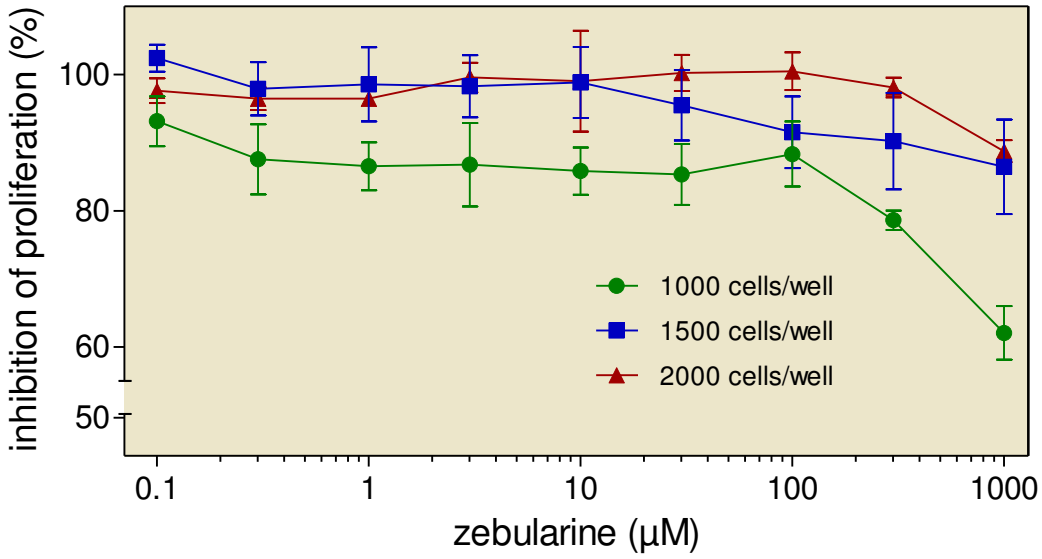

Fig. 13: XTT test for A-498 cells after 5 days of treatment. Cells grown in different quantities per well (1000 cells, 1500 cells, 2000 cells) and treated with different concentrations of zebularine (0 - 0.1 - 0.3 – 1 – 3 – 10 – 30 – 100 – 300 - 1000µM) detected in multi-well spectrophotometer after days of treatment

5.2 Verification of successful demethylation events through expression analysis

Several analysis were carried out to show whether an optimised concentration and duration of zebularine treatment (resulting in the inhibition of de novo methylation of cytosine residues) was successful. Instead of using bisulfite sequencing to show the presence of demethylated C-nucleotides, we chose two indirect assays. In both assessments described below, it is assumed that an arbitrary chosen gene whose expression is switched off by promoter hypermethylation will be upregulated after the treatment with zebularine. This presumed upregulation was measured by:

- qPCR to demonstrate increased levels of mRNA expression (RNA level)
- Western blot analysis to detect an increase in protein expression (protein level)

5.2.1 RNA level

For the RNA level assay, A-498 cells were treated for 5 days with 1000µM zebularine and total RNA was isolated (chapter 4.3)

Two genes that were known to harbour CpG islands were investigated for their upregulation by the treatment (Fig. 14a and b):

- ITGA2 gene (integrin alpha 2), NM_002203
- HMGA2 gene (high mobility group AT-hook 2), NM_003283

Fig. 14: CpG island plot of ITGA2 (a) and HMGA2 (b). The location of the start codon is marked by a red arrow, predicted CpG islands are in boxes

As can be seen from Fig. 14 CpG islands are located around the ATG translation start site in their promoters. Relative gene expression was compared between treated and untreated cell line RNAs using the SYBR Green PCR protocol (Fig. 15, ITGA2 only). The increase of gene expression for both candidates was calculated according ΔΔCt method (Livak and Schmittgen 2001) including efficiency correction as described by Pfaffel et al. (Pfaffl 2001). RGE was calculated by the formula below and by a supportive Excel spreadsheet provided by the following website: http://www.gene-quantification.info/.

*Ratio = $(E1_{target})^{\Delta Ct(control\text{-}treated)}$ $_{\underline{target}}$ / $(E2_{reference})^{\Delta Ct(control\text{-}treated)}$ $_{\underline{reference}}$

As can be deduced from Tab. 15, the transcripts of both genes were upregulated by almost 3 C_t values (from 21.84 to 18.76 for ITGA2, and 20.97 to 18.7 for HMGA2). As expected, the reference gene displayed no variation in expression/regulation in both the treated and untreated cells (data not shown).

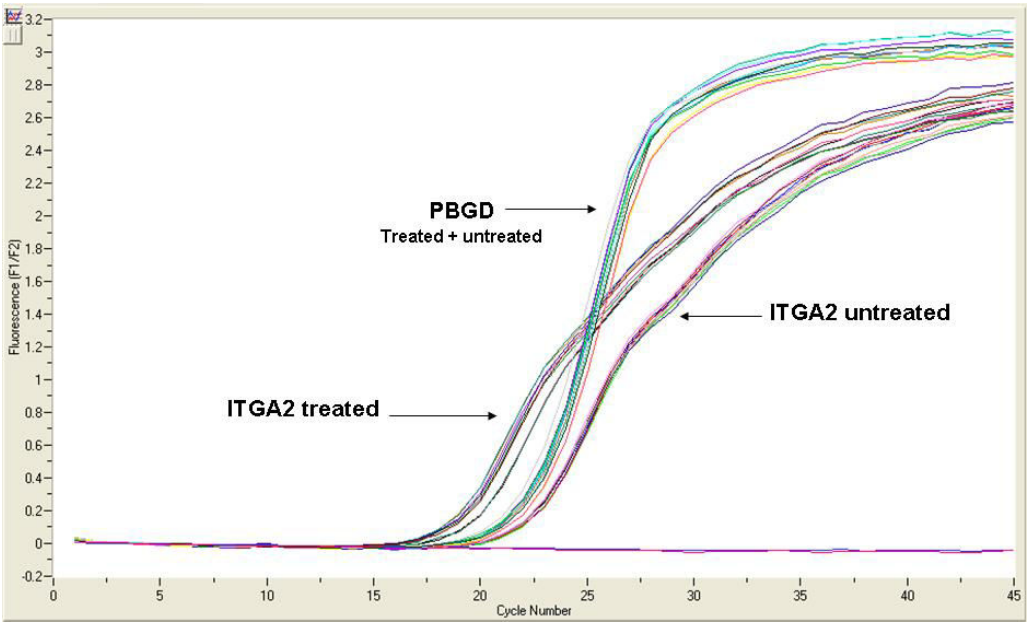

Fig. 15: LightCycler qPCR run for the ITGA2 gene and PBGD reference gene. Higher gene expression for ITGA2 is visualzied by a shift from higher to lower Ct values after zebularine treatment, while reference gene Ct values remain the same in both treated/untreated cells

Tab. 15: RGE calculation for ITGA2 and HMGA2 according Pfaffl et al. (Pfaffl 2001)

		untreated A-498 Control (C)		treated A-498 (T)		target gene	Pfaffel* Top	ref. gene	Pfaffel* Buttom	Ratio
		ref. gene (PBGD)	target	ref. gene (PBGD)	target	C-T	$E1_{(target)}$	C-T	$E2_{(reference)}$	E1/E2
ITGA2	Ex1	22.08	21.99	22.01	19.30	2.69	7.39	0.07	1.05	7.01
	Ex2	22.48	21.75	21.93	18.29	3.46	13.09	0.55	1.51	8.70
	Ex3	22.63	21.79	22.26	18.68	3.11	10.09	0.37	1.32	7.67
	Mean	22.40	21.84	22.07	18.76	3.09	9.94	0.33	1.28	7.78
HMGA2	Ex1	22.08	21.30	22.01	19.58	1.72	4.80	0.07	1.07	4.51
	Ex2	22.48	22.23	21.93	18.65	3.58	26.21	0.55	1.65	5.87
	Mean	22.63	20.97	22.26	18.70	2.27	7.93	0.37	1.40	5.66

The mean upregulation for ITGA2 was around 7.8 folds, whereas the calculated mean average of gene upregulation for HMGA2 was around 5.7 folds.

5.2.2 Protein level

Another proof of the efficacy of zebularine treatment was performed on the protein expression level. We chose the tumor suppressor gene ING1 (inhibitor of growth

family, member 1) also known to harbor multiple CpG islands in its promoter (Fig. 16). A CpG island spans a large region surrounding the ATG translational start codon in the 5´-region of the gene.

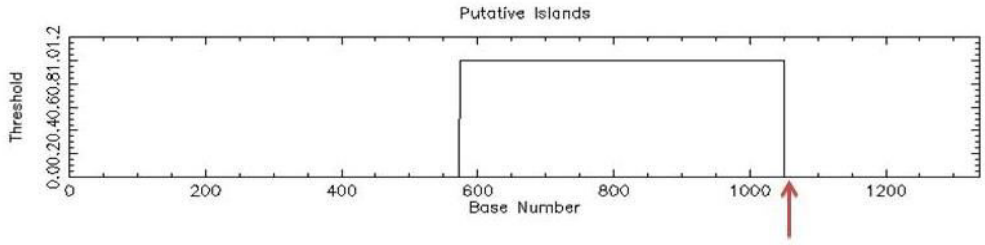

Fig. 16: CpG island plot of ING1. The location of the start codon is marked by a red arrow, predicted CpG islands are in boxes.

Cell lysates of 5-day treated and untreated cells were run on a 12.5% PAGE (see 4.2.3), the gel was blotted onto a PVDF membrane and incubated with a (primary) antibody against ING1 followed by a secondary antibody for detection of the ING1 band protein.

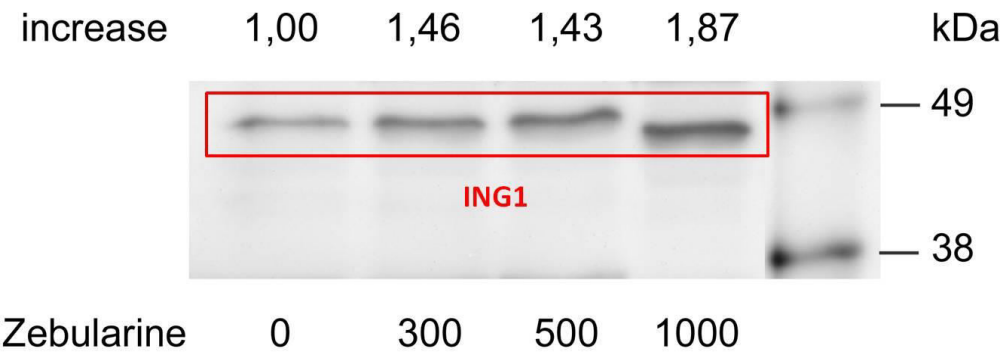

Fig. 17: Western blot analysis of ING1 protein expression after treatment of A-498 cells with different concentrations of zebularine.

The increase of the thickness of the bands was calculated in arbitrary units after densitometric measurements. As shown in Fig. 17 the ING1 protein was differentially expressed at different zebularine concentrations. The ING1-specific band was almost two-fold intense at the 1000µM concentration when compared to the control.

5.3 Transcriptome analysis

High-throughput RNA chip analysis was chosen to get a quantitative overview of the transcriptome expression status in treated and untreated cells. Three independent experiments were carried out in A-498 cells (chapter 4.1). Total RNA from control cells and 1000µM zebularine treated cells was extracted and applied to Affymetrix GeneChip® Human genome U133A 2.0 Array (chapter 4.4) analysis. All microarray data were deposited to the NCBI Geo-database (http://www.ncbi.nlm.nih.gov/geo/) under accession code GSE51627.

18.400 genes were analyzed for expression, whereas apporximately 1000 genes were up- or downregulated at least 1.5-fold after the treatment (Fig. 18).

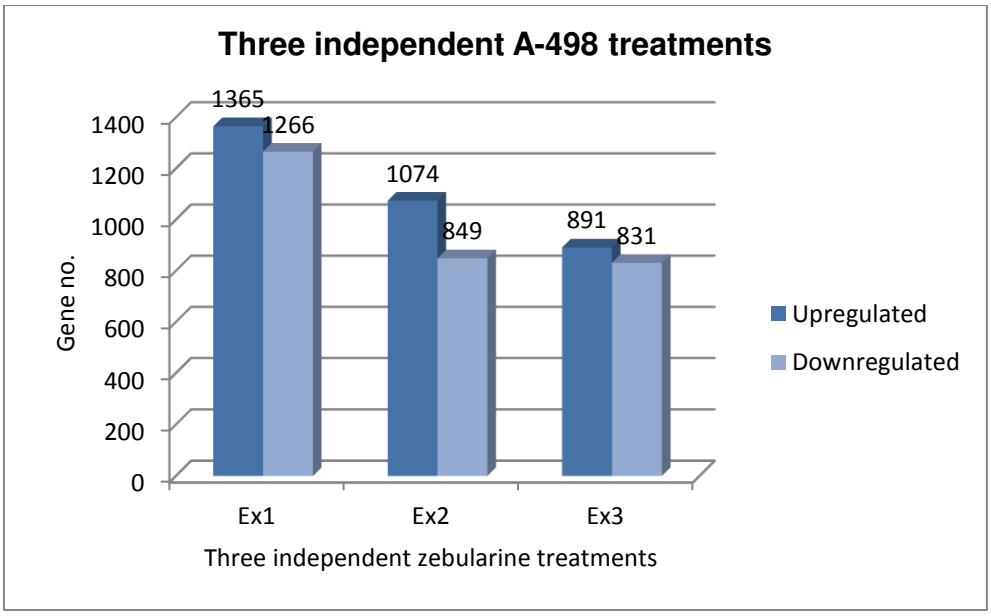

Fig. 18: Upregulated and downregulated genes in three independent zebularine treatments of A-498 cells.

Next we obtained the number of transcripts that were mutually expressed in all three experiments using Venn Diagram. As can be seen in Fig. 19, 308 transcripts were upregulated at least 1.5 fold.

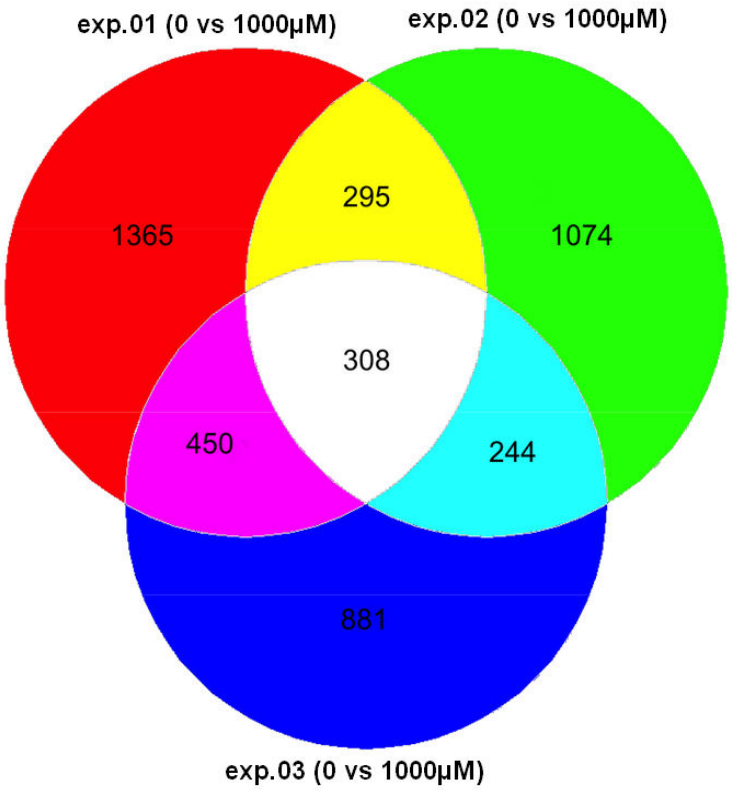

Fig. 19: Venn diagram for three independent biological experiments showing upregulated genes in A-498 cell lines after treatment with the demethylating agent zebularine.

In cases where multiple probe sets specify one particular transcript, the mean value was calculated for that particular transcript. Therefore the number of ≥ 1.5 upregulated transcripts in all three experiments left 264 significantly upregulated transcripts for further examination.

After having assigned the probe sets to particular transcripts we surveyed the Affymetrix website for additional descriptive information of the upregulated genes with regard to: their biological processes involved, their molecular function, and their cellular location (Figs. 20-22). This classification allows for a more functional approach of DNA methylation and its influence on various levels of gene regulation, thus facilitating the interpretation of our findings.

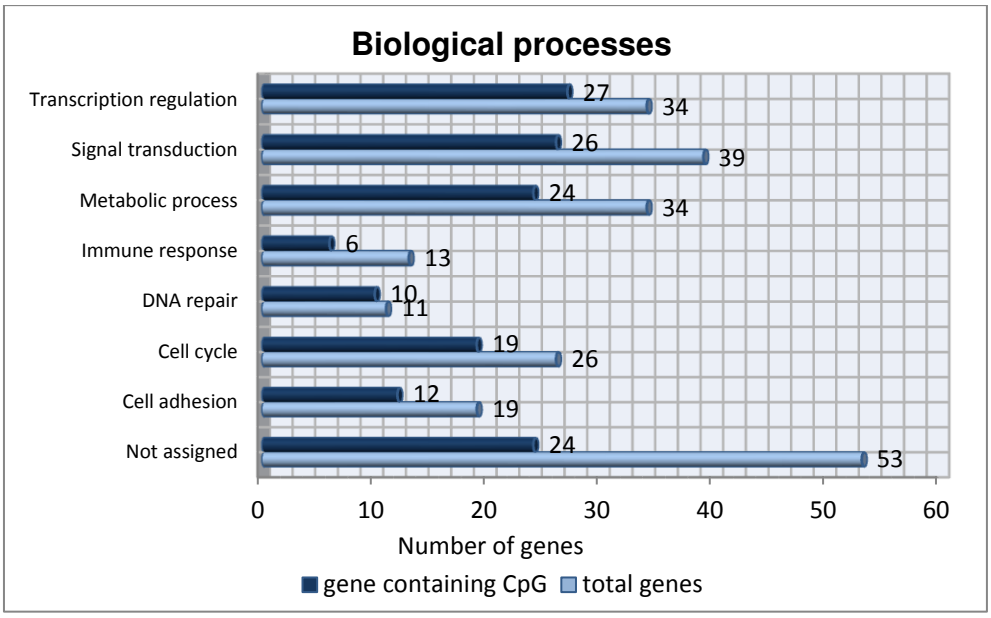

Fig. 20: Upregulated genes classified into eight groups according to their biological processes.

With regard to the biological processes involved, more than 1/3 (n = 99) of the genes belong to the transcription regulation, signal transduction, and cell cycle group, where gene silencing by DNA methylation is experimentally proven (Yoo, Cheng et al. 2004; Alelu-Paz, Ashour et al. 2012). Moreover, 73% (n = 72) of these genes harbor CpG islands in their promoters. In the DNA repair group this number raises up to 90%, which clearly marks genes belonging to this group to be preferentially regulated by promotor hypermethylation and renders them as putative targets for therapeutic intervention (Fig. 20).

When sorted according to their molecular function the metal ion binding protein group was notably high in number (n = 44). 80% of genes within the DNA binding group harbored CpG islands within promoter regions (Fig. 21).

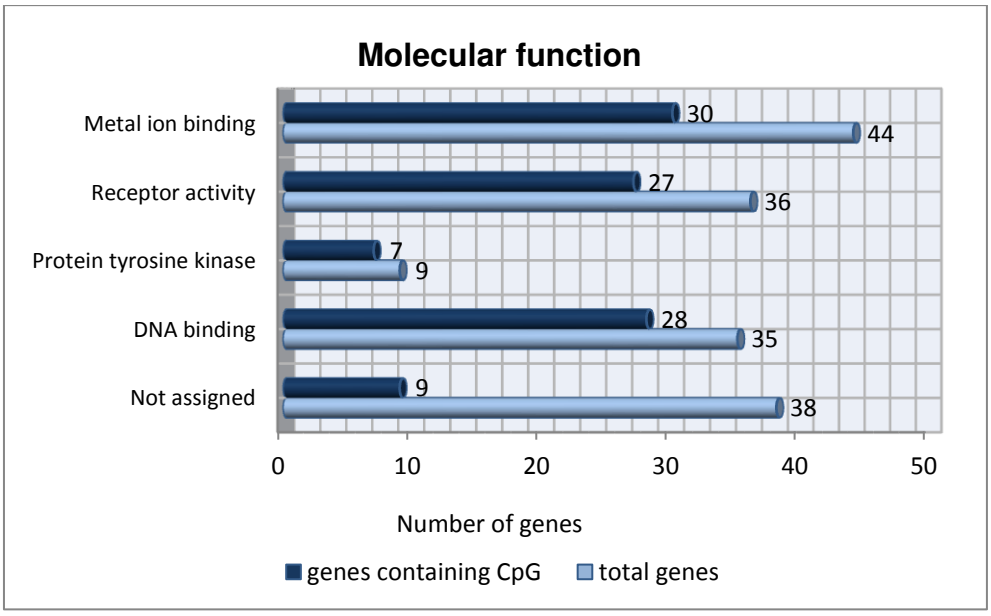

Fig. 21: Upreguated genes classified into six groups according to their molecular function.

Overexpressed genes were also sorted according to their cellular location. The majority of upregulated genes (n = 76) are expressed in the nucleus, which is in concordance with their assumed gene regulatory function on the transcriptional level (Fig. 22).

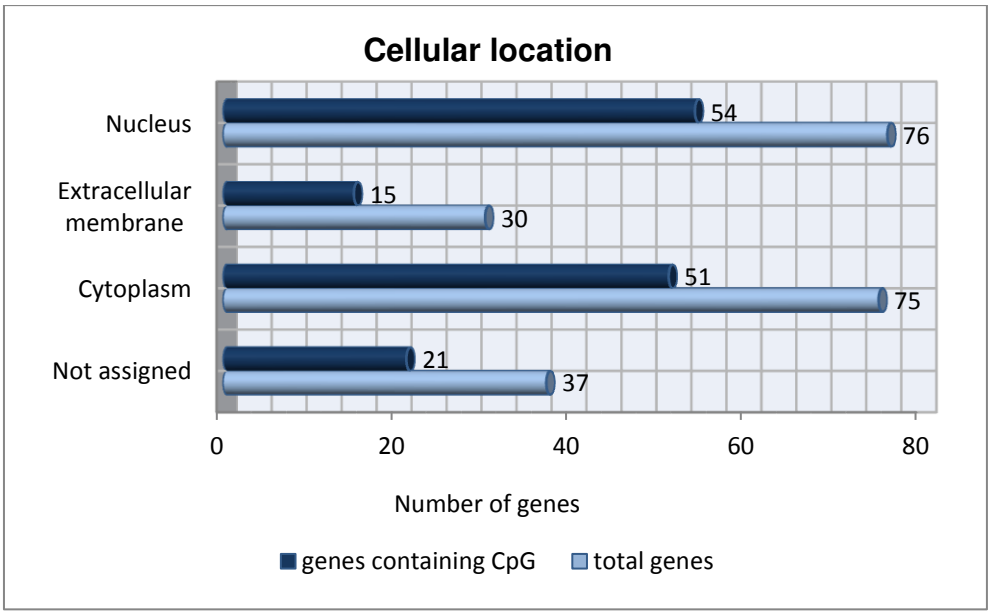

Fig. 22: Upregualted genes classified into four groups according to presence in cellular components.

An almost similar number of transcripts were located in the cytoplasm (n = 75). Such observation could be attributed to various biological / molecular functions as can be expected for signaling transducers (e.g. STAM2) (Takeshita, Arita et al. 1997), kinases (e.g. serine/threonine protein kinases) (Capra, Nuciforo et al. 2006), tumor suppressor proteins (e.g. Ras p21 protein activator 1) (Nath 2005) that participate in regulating cell proliferation and survival.

Furthermore we were interested in knowing the percentage of genes harboring CpG islands. 66% (176/264, Fig. 23) of the upregulated genes contained CpG islands, which is in concordance with our expectations, that the majority of the upregulated genes should possess CpG islands. The one third of upregulated genes that do not harbor CpG islands in their promoter were likely to be upregualed by an unspecific reaction due to genotoxic/cytotoxic stress after the zebularine treatment.

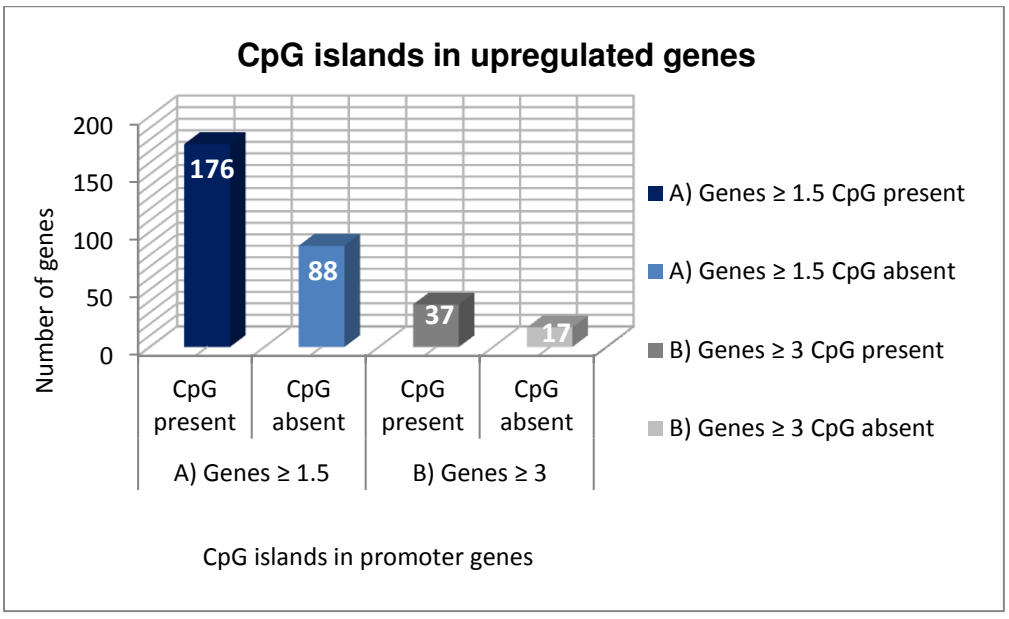

Fig. 23: Determining presence of CpG island: A) >1,5 fold upregulated genes: 66% of total upregulated genes harbored CpG islands. B) >3 fold upregulated genes: 68.5% of total upregulated genes harbored CpG islands.

To further optimize our candidate gene list we applied additional selection criteria. The first criterion for confinement was the restriction to genes that were more than 3-fold upregulated. Hence, the number of genes was further reduced to 54. As a second criterion, those genes were additionally analyzed for the presence of CpG islands in their promoter sequence. This information was obtained from the previous mentioned online EBI-EMBL Tools website.

In this group 68.5% (37/54) harbored at least one CpG island within their promoter. This ratio is in the same range as the overall ratio in the 264 gene group (68.5% vs. 66%). By this confinement, our window of gene selection reduced the genes in number and restrained them to higher efficiency in gene silencing by methylation. The >3 fold upregulated 54 genes are enumerated in Tab. 16 and graphically depicted in Fig. 24.

Tab. 16: Genes upregulated after zebularine cell line treatment. 54 genes sorted as ≥3 fold up-regulation, detected for CpG Islands (CpG island surrounding transcription start site = ✓, CpG island further upstream = ✓✓) and the SAGE Anatomy Viewer ("+" or "++": higer expression in normal tissue, "=": equal expression, "-": lower expression in normal tissue than tumor tissue)

Gene name	Symbol	x-fold Induction	CpG Island *)	The SAGE Anatomy Viewer
inhibin, beta A	INHBA	11.24	NO	=
ephrin-B2	EFNB2	7.87	✓✓	+
tropomodulin 1	TMOD1	7.63	NO	+
secretogranin V	SCG5	7.35	✓	=
tenascin C	TNC	7.3	NO	+
aldehyde dehydrogenase 1 family, member A3	ALDH1A3	5.95	✓	=
collagen, type XIII, alpha 1	COL13A1	5.85	✓	=
plasminogen activator, tissue	PLAT	5.59	NO	++
diacylglycerol kinase, iota	DGKI	5.41	NO	+
acylphosphatase 1	ACYP1	5.38	✓	+
integrin, alpha 2	ITGA2	5.18	✓✓	=
CD44 molecule	CD44	5.1	✓✓	=
progestin and adipoQ receptor family member III	PAQR3	5.05	✓	+
oxysterol binding protein-like 3	OSBPL3	4.67	✓	=
ATP-binding cassette, sub-family G, member 2	ABCG2	4.67	✓	+
metallothionein 2A	MT2A	4.46	✓	++
metallothionein 1X	MT1X	4.44	✓	+
interleukin 1, beta	IL1B	4.41	NO	=
Ras-related associated with diabetes	RRAD	4.18	✓	+
low density lipoprotein receptor-related protein 12	LRP12	4.13	✓	=
sterile alpha motif domain containing 9	SAMD9	4.1	NO	-
potassium intermediate/small conductance calcium-activated channel, subfamily N,member 4	KCNN4	3.95	✓	-
F-box and WD repeat domain containing 7	FBXW7	3.91	NO	+
wingless-related MMTV integration site 5A	WNT5A	3.85	✓	=
metallothionein 1H	MT1H	3.85	✓	No info

apolipoprotein B mRNA editing enzyme catalytic polypeptide-like 3B	APOBEC3B	3.8	NO	-
prolyl 4-hydroxylase, alpha polypeptide II	P4HA2	3.76	✓	-
fatty acid binding protein 6	FABP6	3.72	NO	-
gap junction protein, gamma 1	GJC1	3.7	✓	+
Serglycin	SRGN	3.69	NO	+
RAS p21 protein activator	RASA1	3.65	✓	+
N-acetylgalactosaminyltransferase 2	CSGALNACT2	3.64	✓	+
metallothionein 1G	MT1G	3.62	✓	=
peroxiredoxin 3	PRDX3	3.58	✓	+
CDC-like kinase 1	CLK1	3.58	✓	++
v-ral simian leukemia viral oncogene homolog A	RALA	3.52	✓	++
ubiquitin-like modifier	ISG15	3.5	✓	--
exocyst complex component 5	EXOC5	3.48	✓	+
cytidine deaminase	CDA	3.46	NO	=
Kynureninase	KYNU	3.45	NO	=
aryl hydrocarbon receptor nuclear translocator-like 2	ARNTL2	3.44	✓	=
poliovirus receptor-related 3	PVRL3	3.32	✓	+
ribosomal protein L37a	RPL37A	3.21	NO	-
5'-nucleotidase, ecto	NT5E	3.18	✓	+
ribosomal protein L23a pseudogene 7	RPL23AP7	3.16	NO	+
high mobility group AT-hook 2	HMGA2	3.16	✓✓	+
Melanophilin	MLPH	3.15	✓✓	+
DNA cross-link repair 1B	DCLRE1B	3.15	✓	+
HAUS augmin-like complex, subunit 3	C4orf15	3.15	NO	=
spastic ataxia of Charlevoix-Saguenay (sacsin)	SACS	3.14	NO	=
Transmembrane emp24 domain containing Protein-1	TMED1	3.11	✓	-
DNA repair protein XRCC4	XRCC4	3.02	✓✓	=
AP1 complex segment-2	AP1S2	3.02	✓	+
Serine/threonine Protein Kinase MST4	RP6-213H19.1	3	✓✓	-

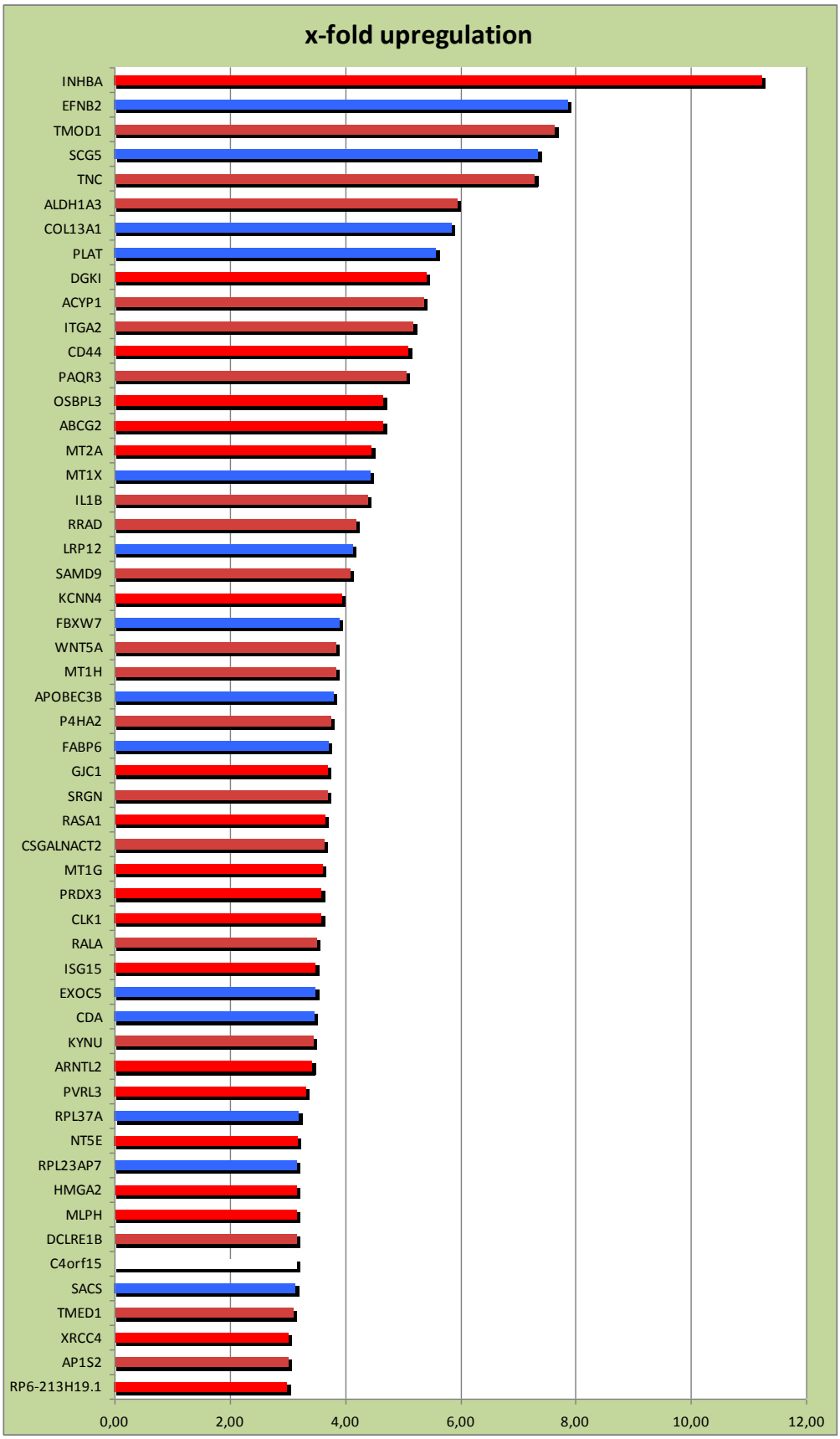

Fig. 24: Intercepted genes reduced (according to ≥3 fold upregulation) to 54 genes and classified according to presence of CpG Islands. Red: CpG near ATG site; light red: CpG away from ATG site; blue: no CpG islands in the gene sequence.

As a third criterion, genes were checked “in silico” for their expression in renal normal and tumor tissues. Genes that were either equally expressed between tissues or display a higher expression in normal tissues were determined as our most likely candidates for detailed expression analysis in patient samples. A typical picture of SAGE analysis (chapter 4.8.2) is displayed in Fig. 25. Genes that were more expressed in normal than in malignant tissue were suspects for methylation.

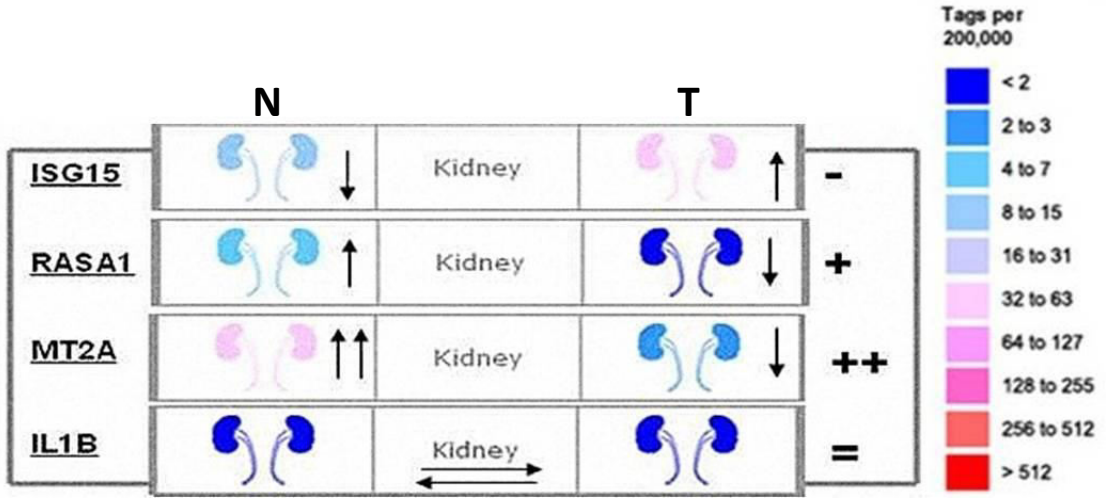

Fig. 25: Example of SAGE Anatomy Viewer analysis for kidney tissue. Relative expression levels are shown in different colors (chapter 4.8.2). Typical examples for the expression of four genes (ISG15, RASA1, MT2A, IL1B) in normal (N) and tumor (T) tissues are given.

5.4 Verification of candidate genes in human renal tissue specimens

After carrying out in vitro experiments and investigating gene upregulation on human cell lines, it was interesting to know how those reactivated genes would behave in tissues of human renal cell carcinoma patients. We were aware that fundamental differences with regard to overall gene expression regulation exists between in vitro culture cells and human isolated tissues. Therefore the transfer of results obtained from in vitro cell cultures to the human tissues must be treated with caution, and any farfetched conclusions with regard to human tumor specimen characterization are at

least inconclusive. For example, the microenvironment that is essential for development of metastases is completely absent in cultured cells (Park, Bissell et al. 2000; Valastyan and Weinberg 2011). In this context, our chosen global demethylation approach with all its restrictions is nevertheless a one of not so many ways to identify genes that may be involved in “methylation-mediated” tumorigenesis (Morris, Ricketts et al. 2011).

5.4.1 Human tissue specimens

The clinical and histopathological data of 49 kidney cancer patients whose tissue specimens were used in this study, are depicted in Tab. 17. Although limited in size, from an epidemiological point of view this study population nevertheless represents a typical caucasian population with regard to gender distribution and the ratio of various histological subtypes. None of these patients received a neo-adjuvant therapy.

Tab. 17: Clinical and histopathological data of RCC patients

		N	%
Samples		49	100
age (years)	35-72		
Median	62.7		
Sex	Male	30	61.2
	Female	19	38.8
Grade	G1	0	-
	G2	29	59.2
	G3	18	36.7
	G4	1	2
	no data	1	2
Stage	pT1	25	51
	pT2	7	14.3
	pT3	17	34.7
distant metastases	Mx	8	16.3
	M0	37	75.5

	M1	4	8.2
lymph node metastases	Nx	15	30.6
	N0	33	67.3
	N1	0	-
	N2	1	2
histological classification			
clear cell carcinoma (ccRCC)		39	79.6
papillary carcinoma, type 1&2 (pRCC)		7	14.3
chromophobic carcinoma (cRCC)		3	6.1

5.4.2 Candidate selection

Eight candidate genes were chosen for further investigation, since earlier reports link their cellular function to processes involved in growth regulation. First and foremost, six of these genes fulfilled our predefined selection criteria (Tab. 18). Two genes that were upregulated less than 3-fold, namely TGM2 and MBD4, were nevertheless added to our analysis since they were well known for their methylation dependent expression in other tumors (see table 19).

Tab. 18: Candidates fold upregulation, CpG islands in promoter and SAGE expression

Genes	Fold upregulation	Presence of CpG (in Promoter seq.)	SAGE Anatomy High expression in kidney
EFNB2	7.87	Yes	+
ITGA2	5.18	Yes	=
RRAD	4.18	Yes	+
MT2A	4.46	Yes	++
MT1H	3.85	Yes	No info
MT1G	3.62	Yes	=
TGM2	1.89	Yes	-
MBD4	1.55	Yes	=

All candidates are TSGs, are methylated in tumor tissues, and contribute to the malignant phenotype in various tumors (Tab. 19).

Tab. 19: Role of candidate genes and their methylation in different cancer tissues

Genes	Chrom. Location	Role as TSG in regulating normal tissue	Methylation in tumor tissue	Reference (Methylation)
EFNB2	13q33	Cell adhesion Angiogenesis Cell differentiation	Colorectal cancer Breast cancer Prostate cancer Leukemia cells	(Alazzouzi, Davalos et al. 2005) (Kuang, Bai et al. 2010) (Noren, Foos et al. 2006)
ITGA2	5q11.2	Cell-cell adhesion Cell migration Differentiation Cell proliferation	Prostate cancer	(James R. Marthick 2011)
RRAD	16q22	Signal transduction (-ve) regulation of cell growth	Lung and breast cancer cell line	(Suzuki, Shigematsu et al. 2007)
TGM2	20q12	Crosslinking components of the extracellular matrix	Glioma Brain tumors	(Dyer, Schooler et al. 2011)
MBD4	3q21.3	DNA and base excision repair (BER)	Colorectal and ovarion cancer	(Howard, Frolov et al. 2009)
MT2A	16q13	Metal binding proteins Metal detoxifiers Scavengers of free radicals	Papillary thyroid and follicular thyroid carcinomas	(Huang, de la Chapelle et al. 2003; Ferrario, Lavagni et al. 2008)
MT1H	16q13	Metal binding proteins Metal detoxifiers Scavengers of free radicals	Haptocellular carcinomas	(Cherian, Jayasurya et al. 2003; Pedersen, Larsen et al. 2009)
MT1G	16q13	Metal binding proteins Metal detoxifiers Scavengers of free radicals	Prostate cancer	(Henrique, Jerónimo et al. 2005)

Candidate genes were verified on paired 49 tissue samples (normal vs tumor), and gene expression between the genes was evaluated.

5.4.3 Individual candidate expression

To our surprise three members of the metallothioneins group showed an exceptional unique expression pattern in human tissues that could not easily be deduced from our in vitro experiments. All of them displayed a remarkable and statistically significant downregulation in tumor tissues when compared to normal tissues.

MT1G showed a distinctive downregulation for gene expression in all measured tumor samples except to one single sample that showed a slight upregulation when compared to normal tissue (Fig. 26). The overall downregulation was 98% (48/49 tissues samples) and the expression difference in gene expression between both tissues was highly significant ($p < 0.0001$).

MT1H behaved similarly, and was detectable however in only 43 paired samples. The six remaining tumor samples were repeated in a second attempt, again values were below the detection limit of the instrument. We assume that these samples were subject to intense methylation (and thus to very low mRNA expression), since those same samples gave reasonable results with our other candidates. Again a remarkable downregulation was found in all the remaining 43 measured samples except with one single sample that showed a slight upregulation (Fig. 26). The overall downregulation for MT1H was also 98% (42/43 tissues samples) and the expression difference in gene expression between both tissues was also highly significant ($p < 0.0001$).

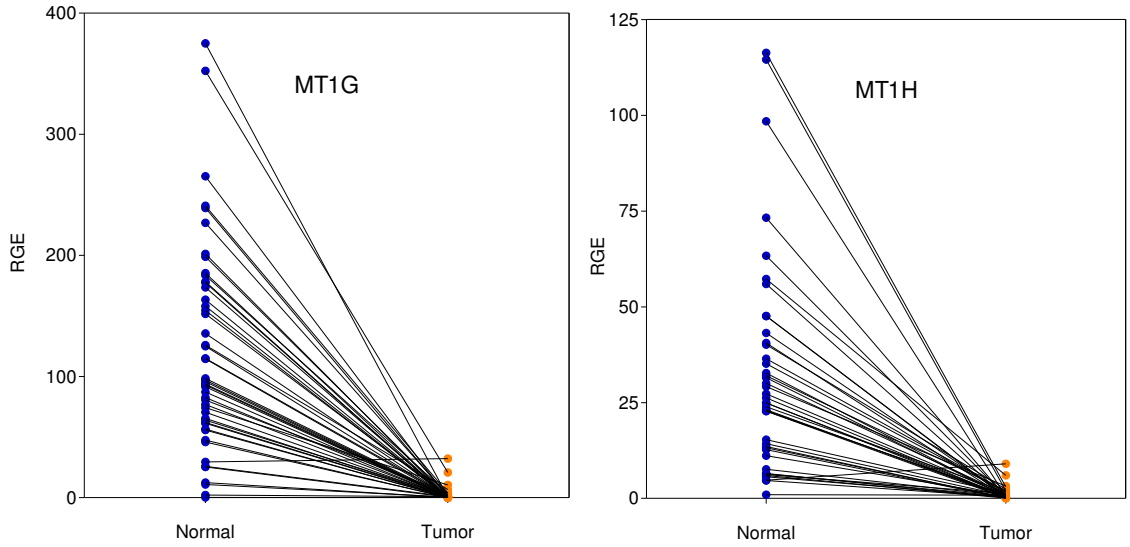

Fig. 26: RGE in paired normal/tumor tissues for MT1G and MT1H.

MT2A as the third candidate of the metallothionein group showed downregulation in 34 tumor tissues and however an upregulation in 15 tumor tissues (Fig. 27).

The overall downregulation was 73% (36/49 tissues samples) and the expression difference between both tissues was found to be significant (p= 0.0013).

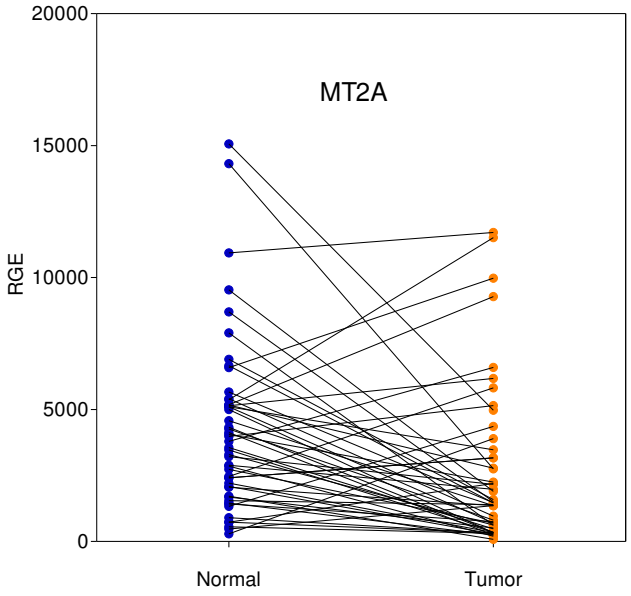

Fig. 27: RGE in paired normal/tumor tissues for MT2A: downregulation vs upregulation.

Further five genes were selected for human tissue interrogation since present scientific knowledge and our in vitro data recommended them as suitable candidates.

Two genes that were highly upregulated after our RNA chip analysis, namely ephrin-B2 (EFNB2, 7.87-fold) and Ras-related associated with diabetes (RRAD, 4.18-fold), displayed unexpectedly higher expression levels in tumor tissues (EFNB2: 32 upregulated/17 downregulated in tumor tissue, p<0.0001; RRAD: 40 upregulated/9 downregulated in tumor tissue, p<0.0002).

Transglutaminase 2 (TGM2) and methyl-CpG binding domain protein 4 (MBD4), both also known to be aberrantly hypermethylated in various cancers, followed the same unexpected pattern after qPCR evaluation in patient samples with 38 upregulated vs. 11 downregulated cases (p<0.0001) for TGM2 and 35 vs. 14 cases (p=0.0028) for MBD4, respectively.

The only candidate transcript that did not reach statstical signifcance (22 upregulated/25 downregulated in tumor tissue, p=0.8756) (Fig. 28) was Integrin alpha 2 (ITGA2, 5.18 fold).

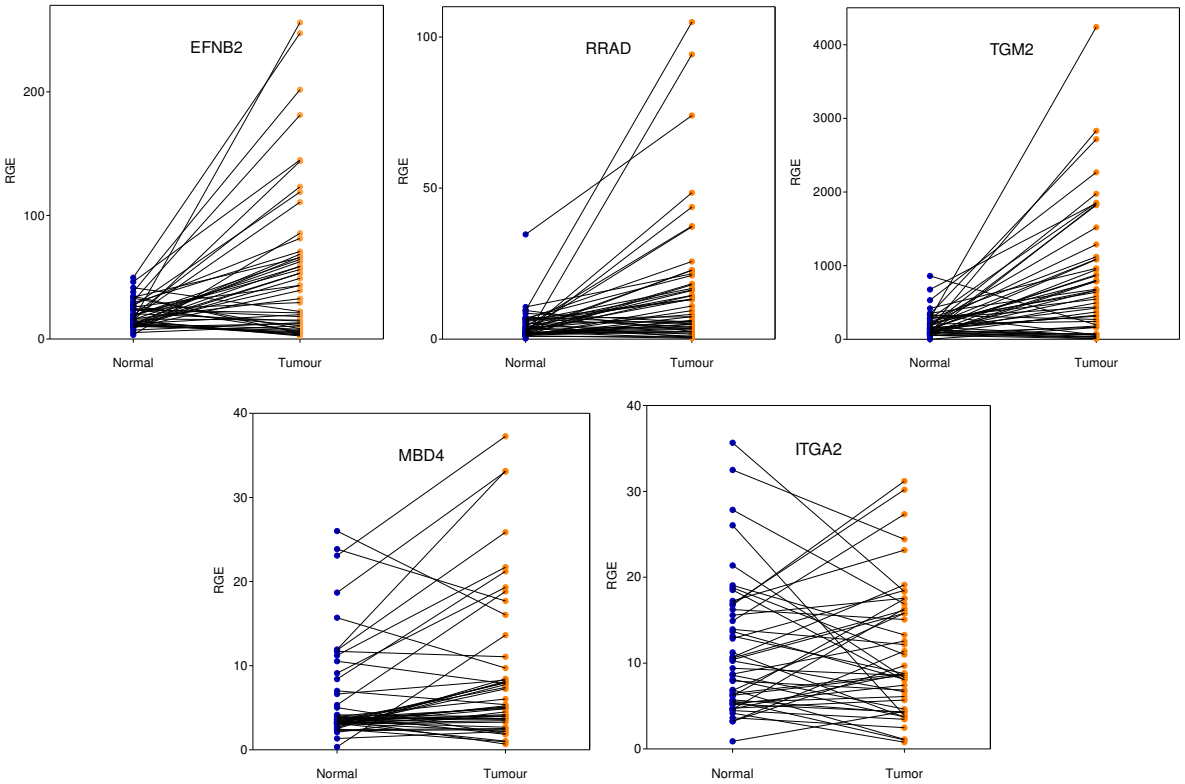

Fig. 28: RGE in paired normal vs tumor tissues for EFNB2, RRAD, TGM2, MBD4, and ITGA2

In summary, only members of the metallothionein group were in concordance with our working hypothesis. The remaining five candidates displayed a mixed expression pattern that excluded them from further consideration Fig. 29.

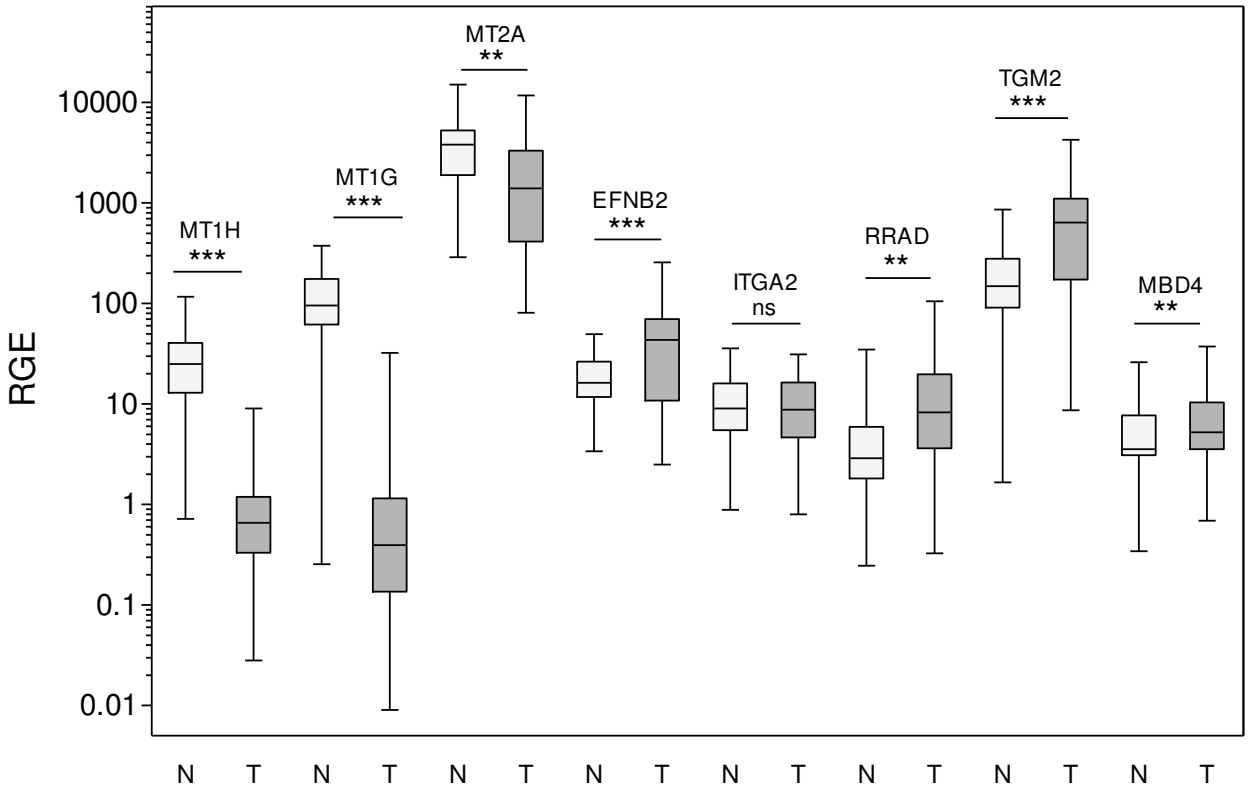

Fig. 29: Box plots for all candidate genes showing expression difference between normal and tumor tissue (*: highly significant; **: significant; ns: no significance).**

5.4.4 Metallothionein expression in relation to clinicopathological data

Tab. 20 summarizes the expression data of the metallothionein genes in relation to clinicopathological data: gender, age, histological RCC subtypes [clear cell RCC, papillary RCC (type 1 & 2), and chromophobe RCC], and tumor grade [Fuhrman grading system (Fuhrman, Lasky et al. 1982)].

Tab. 20: Gene expression profile in patient renal tissue in association with clinicopathologic data (down = downregulation, Up = upregulation)

Patient	Gender	Age	RCC type[1)]	Grade[2)]	pT	pN	M	*MT2A*	*MT1H*	*MT1G*
M_01	M	63	1	3	1a	0	0	down	down	down
M_02	M	50	1	3	1b	0	0	Up	down	down
M_03	F	65	1	2	2	0	0	down	down	down
M_04	F	65	1	2	1b	0	0	Up	down	down
M_06	M	57	1	2	1b	X	X	Up	down	down
M_07	M	55	2	3	3b	0	0	down	down	down
M_08	F	71	2	2	1b	0	0	Up	down	down
M_09	F	58	1	2	1b	0	0	down	-[3)]	down
M_11	M	57	1	2	3b	0	0	down	-	down
M_12	M	57	1	2	1b	0	0	down	down	down
M_13	M	72	1	2	3b	0	0	Up	down	down
M_14	M	46	2	2	1b	X	X	down	down	down
M_16	M	71	1	2	3a	0	0	Up	down	down
M_17	M	74	2	2	1b	0	0	down	down	down
M_18	F	66	2	3	3a	X	0	down	down	down
M_20	M	69	1	2	1b	X	1	down	-	down
M_21	M	62	1	3	1b	0	0	down	down	down
M_22	F	50	1	2	1b	0	0	down	down	down
M_23	F	74	1	3	3a	0	1	Up	down	down
M_25	F	57	1	2	3a	0	0	down	down	down
M_26	M	66	1	2	1b	0	0	down	down	down
M_27	M	65	1	2	1b	X	X	Up	up	Up
M_28	F	59	1	2	1a	0	0	down	down	down
M_29	M	67	2	2	1a	0	0	down	down	down
M_30	F	42	3	2	2a	0	0	down	-	down
M_31	F	70	1	2	3a	0	0	down	down	down
M_32	M	73	1	2	1a	X	0	down	down	down
M_33	M	79	1	3	1a	0	0	down	down	down
M_34	M	62	1	2	3a	0	0	down	down	down
M_35	M	42	2	3	3a	2	1	down	down	down
M_36	M	55	1	3	3a	X	1	down	-	down
M_37	M	43	1	2	2a	0	0	Up	down	down

M_38	M	58	1	2	1a	0	0	Up	down	down
S_01	F	57	3	2	1b	0	0	Up	down	down
S_02	M	59	1	3	3b	0	0	down	-	down
S_03	M	65	1	4	3b	0	X	Up	down	down
S_04	M	62	1	3	1b	0	0	down	down	down
S_05	M	45	1	2	2	X	X	Up	down	down
S_06	M	54	1	3	3b	X	X	down	down	down
S_07	F	75	1	3	2	X	0	down	down	down
S_08	F	69	1	2	3	0	0	down	down	down
S_09	F	35	3	2	2	X	X	down	down	down
S_10	M	77	1	3	1b	X	0	Up	down	down
S_11	M	56	1	2	1a	X	0	down	down	down
S_12	M	60	1	2	1a	X	0	down	down	down
S_13	F	64	1	3	3a	X	X	Up	down	down
S_14	F	76	1	3	1b	0	0	down	down	down
S_15	F	57	1	3	2a	0	0	down	down	down
S_16	F	62	1	3	3a	0	0	down	down	down
P-value								0.0014	<0.0001	<0.0001

[1)] histological subtypes: 1 – clear cell RCC, 2 – papillary RCC (type 1 & 2), 3 – chromophobe RCC

[2)] Fuhrman grading system (Fuhrman, Lasky et al. 1982)

[3)] RGE value(s) below detection limit

In addition we performed a Spearman correlation analysis to assess the statistical significance of the association between MT expression and clinicopahological data. As can be seen from Tab. 21 there was no significant correlation of our expression data to age (at surgery), tumor stage and grade.

The threshold for the age was set by median age. Although we could not see significant correletaion for tumor stage, grade, and age, we found a tendency for a positive correlation between MT2A expression and tumor grading. In addition we found a tendency for negative correlation between MT1G expression and tumor staging.

Tab. 21: Spearman corelation of MTs expression with clinicopathological data

Grading	G1/G2	G3/G4	r*)	P-value
MT1H	25	18	0.03199	0.8997
MT1G	30	19	0.1509	0.5375
MT2A	30	19	0.4123	**0.0794**
Staging				
MT1H	21	22	-0.03636	0.8756
MT1G	25	24	-0.3452	**0.0985**
MT2A	25	24	-0.1722	0.4211
Age				
MT1H	21	22	-0.339	0.1328
MT1G	23	26	0.06028	0.7847
MT2A	23	26	-0.2381	0.2739

5.5 Data comparison to published results

Finally we compared our data to results obtained by other groups. This comparison aims to get a general overview on the quality of our treatment regime with other more frequently used protocols that used DNMT inhibitors like 5-azacytidine and 2-aza-deoxycytidine. Therefore we interrogated published data and compared them to our 308 transcript list (Tab. 22). With one exception and irrespective of the cancer type, our gene list shares at least two or more genes (up to 43) with published data sets. For example, the well-known cell adhesion molecule CD44, is shared in 2 cases of epigenetic screens in renal cancer cell lines and one prostate cancer screen. Transglutaminase 2 (TGM2), which accounts for its involvement in a variety of cellular processes, including adhesion, migration, growth, survival, apoptosis, differentiation, and extracellular matrix organization was upregulated in 3 different cancer types. Thus, as Tab. 22 conveys, the recurring reexpression of a majority of well-characterized CpG-island harboring genes points to a high specificity of the underlying demethylating process no matter which demethylating drug was used.

Tab. 22: Verification of upregulated genes with published data (data from Alkamal, I, at al, 2014, in press)

Author	Cancer	Treatment*)	Cell line(s)	Assay	Gene(s) in common**)
Morris et al.2011 & Morris et al. 2010	Renal cell carcinoma	5- Aza-dC	A498, ACHN, Caki-1, Caki-2, CAL54, KTCL26, 786-O, 769-P, RCC1, RCC4, RCC12, RCC48, SKRC18, SKRC39, SKRC45, SKRC47, UMRC2, UMRC3	Array hybridization (U133A, Affymetrix)	*ARPP-19*, DGKI, ***NBPF10***, ***NBPF8***, RPL37
Ibragimova et al. 2010	Prostate cancer	5- Aza-dC + TSA	DU 145, LNCaP, MDA2b, PC-3	Array hybridization (15K olilgo, MWGBiotech)	*ABCG2*, *ACYP1*, AOC2, *APLP2*, *ATP2B1*, *BRCA2*, ***CD44***, *CD47*, *CD55*, CDC27, *CDC42*, *CLK1*, CYP3A5, ***DGKA***, DGKI, *DSG2*, *DUSP1*, *EFNB2*, ***EIF4A2***, ***IDS***, ***IER5***, IL1B, IL6, INHBA, *ISG15*, LAMB3, ***MCM10***, MKI67, ***NRG1***, OASL, ***PCMT1***, PLAT, PLAUR, ***PLOD3***, ***PTPN12***, RECQL, *RRAD*, SP110, *STC1*, TANK, TGM2, ***UAP1***, *WNT5A*
Ostrow et al.2009	Breast cancer	5- Aza-dC	BT-20, Hs578T, MB-231, MCF-7, MDA- MDA-MB-436	Array hybridization (U133A, Affymetrix)	None
Morris et al.2008	Renal cell carcinoma	5- Aza-dC	Caki-1, KTCL26, 786-0, RCC4, SKRC18, SKRC39, SKRC45, SKRC47, SKRC54, UMRC2, UMRC3	Array hybridization (unspecified)	***CD44***, *ISG15*, SEMA3C
Ibanez de Caceres 2006 et al.	Renal cell carcinoma	5- Aza-dC + TSA	ACHN, HRC51, HRC59, 786-O	Array hybridization (15K olilgo, MWGBiotech)	CDA, ***CD44***, *DUSP1*, ***EIF4A2***, ***IER5***, IL6, INHBA, LAMB3, ***NFE2L3***, ***NRG1***, *P4HA2*, PLAT, PLAUR, ***PLOD3***, *RRAD*, *STC1*, TGM2, ***UAP1***
Lodygin et al. 2005	Prostate cancer	5- Aza-dC + TSA	DU-145, LNCaP, PC-3	Array hybridization (U133A, Affymetrix)	*BRCA2*, *DUSP1*, ***PTGER4***, *SMARCA1*
Yamashita et al. 2002	Esophageal Squamous cell carcinoma	5- Aza-dC + TSA	KYSE10, KYSE30, KYSE70, KYSE140, KYSE150, KYSE200, KYSE410, KYSE520, TE1, TE2, TE3, TE4, TE5, TE7, TE13	Array hybridization (U95Av2, Affymetrix)	*MT1G*, TGM2

*)5- Aza-dC, 2'-Azadesoxycytidine (Decitabine); TSA, trichostatin

)All genes that were upregulated ≥ 1.5 in our experiments were compared to available data. Gene symbol in ***BOLD/Italic:* CpG island in promoter region, gene symbol in *Italic:* canonical CpG island, PLAIN gene symbol: no CpG island present in promoter region

6 Discussion

Based on a well-established functional epigenetic approach (Cheng, Matsen et al. 2003; Andersen, Factor et al. 2010; Ibragimova, Ibanez de Caceres et al. 2010; Mund and Lyko 2010) we present the identification of novel supposedly epigenetically inactivated RCC genes that might be involved in renal tumorigenesis. Furthermore, we provide expression data obtained from RCC patients for the respective transcripts that were marked as candidates by the functional screen in a RCC cell line. Among 54 genes that were re-expressed more than 3-fold after treatment of A-498 cells with moderate doses of the DNMT inhibiting agent zebularine, we focused our attention on genes belonging to the metallothionein (MT) group. In addition, we will discuss the eligibility of our experimental protocol by comparison to published results obtained by similar approaches.

6.1 Downregulation of MTs in renal cell carcinoma

During our functional screen, remarkably members of the MT group displayed expression patterns which were in concordance with our theoretical expectation, i.e. a downregulation in tumor tissues of RCC patients. Three MT genes (MT1G, MT1H, and MT2A) were significantly downregulated in 49 probed RCC patients. Metallothioneins are of particular interest with regard to (renal cell) carcinogenesis since they act as antioxidants thereby protecting against oxidative damage generated by mutagens, antineoplastic drugs, and radiation (Suzuki, Nishimura et al. 2003; Ruttkay-Nedecky, Nejdl et al. 2013).

We observed that MT1G RNA levels were downregulated in 48 of 49 renal tumors. Nguyen et al. previously obtained similar results in 72% of RCC cases by

immunohistochemistry (Nguyen, Jing et al. 2000). Our results are also supported by observations of Dalgin et al., who analyzed promoter hypermethylation of 19 genes in ccRCC and found MT1G among six significantly downregulated genes (Dalgin, Drever et al. 2008). MT1G promoter hypermethylation has been reported in other cancers like hepatocellular carcinoma (Deng, Chakrabarti et al. 1998), colorectal cancer (Stenram, Ohlsson et al. 1999), esophageal cancer (Yamashita, Upadhyay et al. 2002), thyroid cancers (Huang, de la Chapelle et al. 2003) and for prostate carcinomas (Henrique, Jerónimo et al. 2005), too.

Another member of the MT group, namely MT1H, was downregulated in our study in 42 tumor samples; in 6 cases we could not observe any MT1H expression. Two recent studies support our results on MT1H promoter methylation, although in different cancers. Bell et al. analyzed 16 adenoid cystic carcinoma of the salivary gland (ACC) by a combination of microarray analysis and pyrosequencing and marked MT1H as the highest methylated gene among 13 others (Bell, Bell et al. 2011). Furthermore, Han et al. described a putative tumor suppressor function for MT1H by the interplay with euchromatin histone methyltransferase 1 (EHMT1) that itself is abrogated by inactivation of MT1H (Han, Zheng et al. 2013). They found a 10-100-fold decrease in MT1H expression due to promoter hypermethylation in prostate and liver tumors when compared to normal tissues, in line with our results on renal tumors.

The third candidate, MT2A, is downregulated in 34 cases of RCC tissues, and upregulated in the remaining 13 tissues. This observation is in contrast to 2-fold upregulation described by Nguyen et al. on a limited number of 11 RCC patients through qPCR analysis and immunohistochemistry (Nguyen, Jing et al. 2000) and may be due to a more complex regulation of this particular gene. It is noteworthy that this group also found isoforms MT1A and MT1G to be downregulated in their RCC

samples. In colorectal cancers and respective cell lines, MT2A is downregulated up to 27-fold when compared to normal counterparts (Zhang, Zhou et al. 1997). Downregulation of MT2A was also demonstrated as a key element in the immortalization of human cells after knockout experiments (Duncan 1999).

Since there are many known cancer instances where MT expression is increased, the expression status of MT genes in human tumors is not universal and may depend on additional factors like differentiation status and proliferation index, among others (Cherian, Jayasurya et al. 2003). In summary, still limited and sometimes contradictory expression data were reported on the contribution of various MT isoforms in certain cancer types (Pedersen, Larsen et al. 2009). Due to the small sample size of our patient group, we were not able to provide reliable associations between different MTs isoforms and tumor grade/stage, therapy resistance, and prognosis, respectively. Therefore we suggest an extended investigation on the role of MT genes in a larger RCC cohort to finally clarify the contribution of MTs in renal carcinogenesis. In parallel we propose an assessment of MTs as potential non-invasive biomarkers (blood, urine) for the clinical management of RCC.

6.2 Role of MTs as potential tumor suppressors

Metallothioneins are of particular interest with regard to (renal cell) carcinogenesis since they act as antioxidants protecting DNA against oxidative damage generated by mutagens, antineoplastic drugs, and radiation (Suzuki, Nishimura et al. 2003). The elucidation of molecular functions of various MT isoforms that substanciate their tumor suppressor role in various signaling pathways and different cancers is still in its beginning. According to Fu et. al., restoring of MT1G in thyroid cancer cells decreased the expression of MDM2 (usually phophorylated and overexpressed

through the PI3K/Akt pathway), and thus increased the stability of p53 and its downstream targets (p21, Bak, and Smac). Likewise, ectopic expression of MT1G also upregulates E-cadherin, thus inhibiting cell migration and invasion. Furthermore, this restoration prevented the phosphorylation and consequent degradation of Rb, the gatekeeper of cell-cycle progression (Fu 2013).

The most intriguing functions of MTs are related to their metal-binding activity, including detoxification of heavy metals, protecting against oxidative stress, and being reservoirs and donators of zinc to certain enzymes and transcription factors (Fu, Lv et al. 2013).

Zn inhibits the formation of the reactive free radical superoxide anion through NADPH oxidase, induces metallothionines as free radical scavengers, and acts as integral metals of the antioxidant superoxide dismutases (SOD) (Jomova and Valko 2011). This subsequently prevents the formation of reactive oxygen species (ROS) that functionally activate NF-κB. NF-κB itself is a protein complex that activates growth factors, antiapoptotic molecules, and proto-oncogenes (like bcl-2, c-myc, TNF receptor associated factor 1) (Krizkova, Ryvolova et al. 2012) leading finally to enhanced proliferation and tumorigenesis, inflammatory cytokines and adhesion molecules (Fig. 30). Moreover, Zn reduces the production of inflammatory cytokines through upregulating the zinc-finger A20 protein thus inhibiting NF-κB via TRAF pathway (Jomova and Valko 2011). In this context, overexpression of MT in various cancer cell lines increased the mRNA and protein expression of the NF-κB inhibitor (IκB-α) and thus reduced the DNA binding activity of NF-κB in the nucleus. However, opposite findings were reported in endogenous MT knockdown experiments, namely MT2A (Pan, Huang et al. 2013).

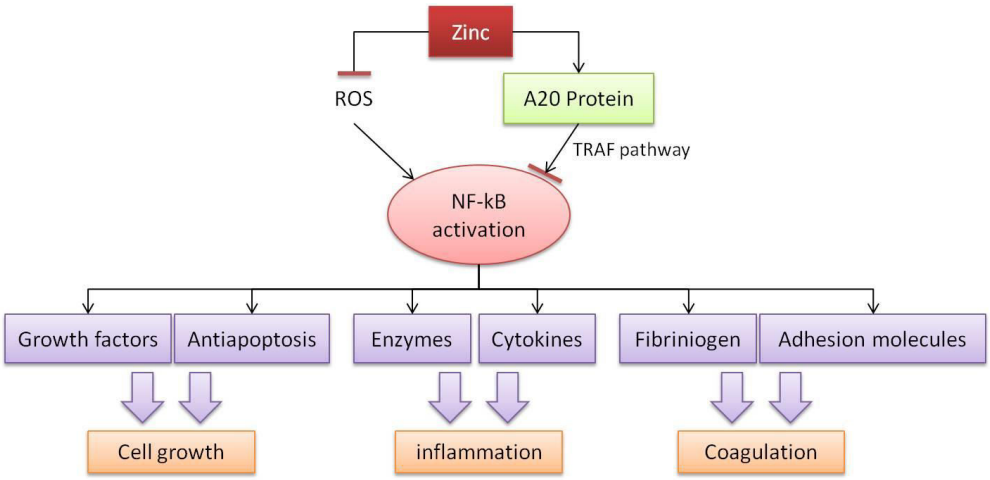

Fig. 30: The role of zinc as an antiinflammatory and antioxidant [Adjusted from (Jomova and Valko 2011)]

As zinc dependent enzymes, DNA and RNA polymerases that contain zinc finger domains depend on Zn as an essential structure modulator. In this context, it is possible that with increasing tumor grade in RCC, transcription and translation may be disrupted due to a gradual decline in zinc storage and subsequent decrease in MT that finally leads to altered growth and differentiation (Izawa, Moussa et al. 1998).

MT expression localizes to the nucleus in cells entering cell cycle and reaches maximal levels during G1/S transition phase where the requirement of zinc is highest (Fan and Cherian 2002). In this respect, MTI and MTII expression was described to activate various metalloenzymes and transcription factors which are cell-cycle regulated, peaking near the G1/S boundary, and which are required for DNA synthesis, cell regeneration and tissue repair (Krizkova, Ryvolova et al. 2012). As immunomodulatory factors in central nervous system, MTs were shown to stimulate the expression of anti-inflammatory cytokines, growth factors, neurotrophins and their receptors, promoting cell survival and regeneration (Pedersen, Larsen et al. 2009).

Sato and coworkers stated that MT's low affinity for zinc and high affinities for toxic heavy metals like Cd and Hg, pointed out to MT's role as heavy metal detoxifiers (Sato and Kondoh 2002). Furthermore, levels of both biomarkers of DNA damage,

p53 and p21, were significantly increased at initial stages of DMBA-induced tumors in MT-knockout mice. This suggests that endogenous MT expression prevents the DMBA-caused DNA damage and confirming the anticarcinogenic role for MTs in suppressing mutation induction at the initial phase of tumorigenesis (Palmiter 1998; Suzuki, Nishimura et al. 2003).

Zinc binding is reported to be crucial for p53 stabilization and DNA binding (Fan and Cherian 2002). Since MTs play a critical role in zinc uptake, distribution, storage, and release, they are also most likely involved in the stabilisation and maintainance of optimal activity of transcription factors such as HIF-1α. (Eid, Géczi et al. 1998; Fan and Cherian 2002; Cherian, Jayasurya et al. 2003). For example, Nardinocchi et al. were able to show, that zinc indeed downregulated HIF-1α protein levels in human prostate cancer and glioblastoma cell lines under hypoxia (Nardinocchi, Pantisano et al. 2010). Moreover, Kojima et al. linked hypoxia-induced upregulated MT expression patterns to chronic kidney injury, thereby connecting MT expression closely to the pVHL- HIF-1α pathway (Kojima, Tanaka et al. 2009). Taken together these observations can be interpreted as a cellular defense mechanism against hypoxic conditions and as a readjustment to normoxia.

6.3 Validation of further candidates

In addition to the MT transcripts, further five candidates were validated in RCC patients (Fig. 29). Although those genes were upregulated in our in vitro screen, they did not display the expected downregulation in RCC tissues. Furthermore the presence of CpG islands suggested a methylation-dependent regulation. The absence of their expected downregulation in tumor tissues may be explained by additional regulatory mechanisms that were missing in our in vitro screen (e.g.

stromal interaction, the presence of an immune system, etc.). Another reason that may explain the upregulation in the cell line may be attributed to genotoxic stress due to the action of the DNMT inhibitor (Patra, Deb et al. 2011; Ruiz-Magana, Rodriguez-Vargas et al. 2012). Therefore we excluded these five transcripts from further consideration in this study.

6.4 Validating the consistency of our demethylating approach

For obvious reasons, we were interested in the consistency of our approach when compared to published results using a similar experimental design. Therefore we compared our initial 308 transcript list to publicly available data (Tab. 22). With regard to functional processes in kidney physiology and tumorigenesis, our epigenetic screen revealed well-known kidney cancer or at least cancer-specific genes (Tab. 16). Among them are the metastasis suppressor CD44 (5,1-fold upregulated), stanniocalcin 1 (STC1; 2,14-fold) and collagen type 13A1 (COL13A1; 5,85-fold). A close relative of COL13A1, COL14A1, was shown by Morris et al. to be associated with a poorer prognosis in RCCs independent of tumor size, stage or grade (Morris and Maher 2010). STC1 is a glycoprotein that is involved in renal calcium and phosphate homeostasis and recently gained attraction as a biomarker for several other cancers like gastric, colorectal, lung, ovary, and esophageal cancers (Yeung, Law et al. 2012). In addition, Tab. 22 conveys that the recurring reexpression in our experiments of a majority of well-characterized CpG-island harboring genes points to a high specificity of the underlying demethylating process.

6.5 Conclusion

Although a possible contribution of metallothioneins to renal cell carcinogenesis is not fully understood (Cherian, Jayasurya et al. 2003), our discovery of an almost exclusively downregulation of selected MT genes in RCC tissues emphasizes a plausible link between a deregulated metabolism and tumor development.

Acknowledging the hypothesis that kidney cancer is fundamentally a metabolic disorder whose essential cancer genes (e.g. VHL, MET, BDH, FH, SDH, TSC1/2) play major roles in energy, nutrient, iron, and oxygen sensing (Linehan, Bratslavsky et al. 2010), it is of particular interest that our screen revealed members of the physiologically related MT group as turned-off genes. Should further investigations strengthen the role of MTs in kidney physiology, they may be considered for a targeted intervention during dysregulated kidney development and renal carcinogenesis.

In the context of an ever-increasing demand for suitable markers for early detection and clinical decision-making, selected members of the MT group may also be considered as future putative biomarkers for renal cell carcinomas.

7 Summary/Zusammenfassung

7.1 Summary

Transcriptional silencing associated with aberrant promotor methylation is acknowledged as a common mechanism for loss of function of tumor suppressor genes in cancer cells.

This thesis describes an epigenetic screen aimed to discover hitherto unkown genes that are silenced by this mechanism in kidney cancer. Reexpressed genes were analyzed in the kidney cancer cell line A-498 after treatment with the DNA methyltransferase (DNMT) inhibitor zebularine. Transcript expression changes in treated and untreated cells were compared using Affymetrix GeneChip® Human genome U133A 2.0 Arrays. For candidate selection we applied criteria like the presence of CpG islands and SAGE-database derived expression data. 308 transcripts were shown to be upregualted ≥ 1.5-fold after the combination of three individual experiments. We also included experiments to show the efficacy of the demethylation treatment.

Eight candidates were further investigated for their hypothesized downregulation in 49 patient RCC tumor tissues. A significant downregulation for three members of the metallothioneins was detected, with an overall percentage of 98% in cases for both MT1G and MT1H, and 73% for MT2A.

We could not demonstrate a statistical significant correlation of this downregulation to clinicopathological characteristics like tumor stage and grade. At least we found a tendency for a positive correlation between MT2A expression and grading. In addition we found a tendency for negative correlation between MT1G expression and tumor staging.

We deposited the results of our RNA chip analysis to the Geo-database (accession code GSE51627) and compared our initial 308 transcript list to publicly available data. This comparison revealed a shared number of well-known kidney cancer genes that points to a high specificity of the underlying demethylating process no matter which demethylating drug was used and speaks for the consistency of our experimental apporach.

7.2 Zusammenfassung

Transkriptionsinaktivierung vorgerufen durch eine veränderte Promotormethylierung ist ein akzeptierter Mechanismus für den Funktionsverlust von Tumorsuppressorgenen.

Die vorliegende Arbeit beschreibt ein epigenetisches Screening-Verfahren zu Entdeckung bislang unbekannte Gene beim Nierenzellkarzinom, die durch diesen Mekanismus inaktiviert wurden.

Wir untersuchten reaktivierte Gene nach der Behandlung der Nierenzellkarzinom-Zelllinie A-498 mit den DNA methyltransferase (DNMT) Inhibitor Zebularine. Expressionsveränderungen in behandelten und unbehandelten Zellen wurden durch den Einsatz von Affymetrix GeneChip® Human genome U133A 2.0 Arrays analysiert. Für die Kandidatenselektion wurden Kriterien wie das Vorhandensein von CpG Inseln und Expressionsdaten der SAGE-Datenbank verwendet. 308 Transkripte waren nach der kombinierten Analyse von drei Einzelexperimeten mehr als 1.5-fach hochreguliert. In zusätzlichen Experimenten wurde die Wirksamkeit der Demethylierung durch Zebularine untersucht.

Acht Kandidaten wurden für den Nachweis eine veringerten Expression entsprechend unsere Arbeithypothese in 49 Tumorgeweben von Nierenzellkarzinom-

Tumorpatienten weiter analysiert. Wir fanden ein signifikant veringerte Expression für drei Metallothionein-Gene in 98% aller Fälle für MT1G und MT1H, und 73% aller Fälle für MT2A.

Wir konnten keine statistische signifikante Korrelation dieser verminderte Expression mit klinish-pathologischen Eigenschaften wie dem Tumorstadium und dem Tumorgrad nachweisen. Wir fanden eine Tendenz für eine positive Korrelation zwischen der MT2A Expression und dem Tumorgrad, so wie eine Tendenz zur negativen Korrelation der MT1G expression mit dem Tumorstadium.

Die Resultate der RNA Chip-Analysen wurden and die Geo-Datenbank übermittelt (accession code GSE51627). Die Liste der 308 Transkripte wurde mit öffentlich zugänglichen Daten verglichen. Dieser Vergleich ergab Übereinstimmungen mit bekannten Nierenzellkarzinom-Genen, die auf eine hohe Spezifität des zugrunde liegenden Demethylierungs-Verfahrens schließen lassen, was nicht zuletzt für die Konsistenz des experimentallen Vorgehens spricht.

8 References

Alazzouzi, H., V. Davalos, et al. (2005). "Mechanisms of Inactivation of the Receptor Tyrosine Kinase EPHB2 in Colorectal Tumors." Cancer Research **65**(22): 10170-10173.

Alelu-Paz, R., N. Ashour, et al. (2012). "DNA methylation, histone modifications, and signal transduction pathways: a close relationship in malignant gliomas pathophysiology." J Signal Transduct **2012**: 956958.

Andersen, J. B., V. M. Factor, et al. (2010). "An integrated genomic and epigenomic approach predicts therapeutic response to zebularine in human liver cancer." Sci Transl Med **2**(54): 54ra77.

Arai, E. and Y. Kanai (2010). "Genetic and epigenetic alterations during renal carcinogenesis." International journal of clinical and experimental pathology **4**(1): 58-73.

Beisler, J. A. (1978). "Isolation, characterization, and properties of a labile hydrolysis product of the antitumor nucleoside, 5-azacytidine." J Med Chem **21**(2): 204-8.

Bell, A., D. Bell, et al. (2011). "CpG island methylation profiling in human salivary gland adenoid cystic carcinoma." Cancer **117**(13): 2898-909.

Berdasco, M. and M. Esteller (2010). "Aberrant Epigenetic Landscape in Cancer: How Cellular Identity Goes Awry." Developmental cell **19**(5): 698-711.

Bergstrom, A., C. C. Hsieh, et al. (2001). "Obesity and renal cell cancer--a quantitative review." Br J Cancer **85**(7): 984-90.

Bhatt, A. N., R. Mathur, et al. (2010). "Cancer biomarkers - current perspectives." Indian J Med Res **132**: 129-49.

Boon, K., E. C. Osorio, et al. (2002). "An anatomy of normal and malignant gene expression." Proc Natl Acad Sci U S A **99**(17): 11287-92.

Burrell, R. A., N. McGranahan, et al. (2013). "The causes and consequences of genetic heterogeneity in cancer evolution." Nature **501**(7467): 338-45.

Cairns, P. (2007). "Gene methylation and early detection of genitourinary cancer: the road ahead." Nat Rev Cancer **7**(7): 531-43.

Cancer Genome Atlas Research, N. (2013). "Comprehensive molecular characterization of clear cell renal cell carcinoma." Nature **499**(7456): 43-9.

Capra, M., P. G. Nuciforo, et al. (2006). "Frequent alterations in the expression of serine/threonine kinases in human cancers." Cancer Res **66**(16): 8147-54.

Champion, C., D. Guianvarc'h, et al. (2010). "Mechanistic insights on the inhibition of c5 DNA methyltransferases by zebularine." PLoS One **5**(8): e12388.

Chen, J., W.-O. Lui, et al. (2003). "The t(1;3) breakpoint-spanning genes LSAMP and NORE1 are involved in clear cell renal cell carcinomas." Cancer Cell **4**(5): 405-413.

Cheng, J. C., C. B. Matsen, et al. (2003). "Inhibition of DNA Methylation and Reactivation of Silenced Genes by Zebularine." Journal of the National Cancer Institute **95**(5): 399-409.

Cheng, J. C., C. B. Yoo, et al. (2004). "Preferential response of cancer cells to zebularine." Cancer Cell **6**(2): 151-8.

Cherian, M. G., A. Jayasurya, et al. (2003). "Metallothioneins in human tumors and potential roles in carcinogenesis." Mutat Res **533**(1-2): 201-9.

Christoph, F., S. Weikert, et al. (2006). "Promoter Hypermethylation Profile of Kidney Cancer with New Proapoptotic p53 Target Genes and Clinical Implications." Clinical Cancer Research **12**(17): 5040-5046.

Clague, J., J. Lin, et al. (2009). "Family history and risk of renal cell carcinoma: results from a case-control study and systematic meta-analysis." Cancer Epidemiol Biomarkers Prev **18**(3): 801-7.

Clifford, S. C., A. H. Prowse, et al. (1998). "Inactivation of the von Hippel–Lindau (VHL) tumour suppressor gene and allelic losses at chromosome arm 3p in primary renal cell carcinoma: Evidence for a VHL-independent pathway in clear cell renal tumourigenesis." Genes, Chromosomes and Cancer **22**(3): 200-209.

Cohen, H. T. and F. J. McGovern (2005). "Renal-cell carcinoma." The New England journal of medicine **353**(23): 2477-90.
Costa, V., R. Henrique, et al. (2007). "Quantitative promoter methylation analysis of multiple cancer-related genes in renal cell tumors." BMC Cancer **7**(1): 133.
Dalgin, G. S., M. Drever, et al. (2008). "Identification of novel epigenetic markers for clear cell renal cell carcinoma." J Urol **180**(3): 1126-30.
Dalgliesh, G. L., K. Furge, et al. (2010). "Systematic sequencing of renal carcinoma reveals inactivation of histone modifying genes." Nature **463**(7279): 360-363.
Das, P. M. and R. Singal (2004). "DNA methylation and cancer." J Clin Oncol **22**(22): 4632-42.
Deng, D. X., S. Chakrabarti, et al. (1998). "Metallothionein and apoptosis in primary human hepatocellular carcinoma and metastatic adenocarcinoma." Histopathology **32**(4): 340-7.
Dhillon, V. S., A. R. Young, et al. (2004). "Promoter hypermethylation of MGMT, CDH1, RAR-beta and SYK tumour suppressor genes in granulosa cell tumours (GCTs) of ovarian origin." British journal of cancer **90**(4): 874-81.
Dulaimi, E., I. I. de Caceres, et al. (2004). "Promoter Hypermethylation Profile of Kidney Cancer." Clinical Cancer Research **10**(12): 3972-3979.
Duncan, E. L. (1999). "Downregulation of metallothionein-IIA expression occurs at immortalization." Oncogene **18**(4): 897-903.
Dyer, L. M., K. P. Schooler, et al. (2011). "The transglutaminase 2 gene is aberrantly hypermethylated in glioma." J Neurooncol **101**(3): 429-40.
Egger, G., G. Liang, et al. (2004). "Epigenetics in human disease and prospects for epigenetic therapy." Nature **429**(6990): 457-63.
Eid, H., L. Géczi, et al. (1998). "Do metallothioneins affect the response to treatment in testis cancers?" Journal of Cancer Research and Clinical Oncology **124**(1): 31-36.
Esteller, M. (2002). "CpG island hypermethylation and tumor suppressor genes: a booming present, a brighter future." Oncogene **21**(35): 5427-40.
Esteller, M. (2007). "Cancer epigenomics: DNA methylomes and histone-modification maps." Nat Rev Genet **8**(4): 286-298.
Esteller, M. (2008). "Epigenetics in Cancer." New England Journal of Medicine **358**(11): 1148-1159.
Esteller, M., P. G. Corn, et al. (2001). "A gene hypermethylation profile of human cancer." Cancer Res **61**(8): 3225-9.
Fan, L. Z. and M. G. Cherian (2002). "Potential role of p53 on metallothionein induction in human epithelial breast cancer cells." Br J Cancer **87**(9): 1019-26.
Ferlay, J., H. R. Shin, et al. (2010). GLOBOCAN 2008 v2.0, Cancer Incidence and Mortality Worldwide: IARC CancerBase No. 10 [Internet]. Lyon, France, International Agency for Research on Cancer.
Ferrario, C., P. Lavagni, et al. (2008). "Metallothionein 1G acts as an oncosupressor in papillary thyroid carcinoma." Laboratory investigation; a journal of technical methods and pathology **88**(5): 474-481.
Fu, J., H. Lv, et al. (2013). "Metallothionein 1G functions as a tumor suppressor in thyroid cancer through modulating the PI3K/Akt signaling pathway." BMC Cancer **13**: 462.
Fuhrman, S. A., L. C. Lasky, et al. (1982). "Prognostic significance of morphologic parameters in renal cell carcinoma." The American Journal of Surgical Pathology **6**(7): 655-664.
Gerlinger, M., S. Horswell, et al. (2014). "Genomic architecture and evolution of clear cell renal cell carcinomas defined by multiregion sequencing." Nat Genet **46**(3): 225-33.
Gerlinger, M., A. J. Rowan, et al. (2012). "Intratumor heterogeneity and branched evolution revealed by multiregion sequencing." N Engl J Med **366**(10): 883-92.
Gnarra, J. R., K. Tory, et al. (1994). "Mutations of the VHL tumour suppressor gene in renal carcinoma." Nat Genet **7**(1): 85-90.
Greger, V., E. Passarge, et al. (1989). "Epigenetic changes may contribute to the formation and spontaneous regression of retinoblastoma." Human Genetics **83**(2): 155-158.

Han, Y. C., Z. L. Zheng, et al. (2013). "Metallothionein 1h Tumor Suppressor Activity in Prostate Cancer Is Mediated By Euchromatin Methyltransferase 1." J Pathol.

Hanahan, D. and R. A. Weinberg (2011). "Hallmarks of cancer: the next generation." Cell **144**(5): 646-74.

Hartwell, L., D. Mankoff, et al. (2006). "Cancer biomarkers: a systems approach." Nat Biotechnol **24**(8): 905-8.

Henrique, R., C. Jerónimo, et al. (2005). "MT1G Hypermethylation Is Associated with Higher Tumor Stage in Prostate Cancer." Cancer Epidemiology Biomarkers & Prevention **14**(5): 1274-1278.

Herman, J. G., F. Latif, et al. (1994). "Silencing of the VHL tumor-suppressor gene by DNA methylation in renal carcinoma." Proceedings of the National Academy of Sciences **91**(21): 9700-9704.

Herman, J. G., A. Merlo, et al. (1995). "Inactivation of the CDKN2/p16/MTS1 Gene Is Frequently Associated with Aberrant DNA Methylation in All Common Human Cancers." Cancer Research **55**(20): 4525-4530.

Herranz, M., J. Martin-Caballero, et al. (2006). "The novel DNA methylation inhibitor zebularine is effective against the development of murine T-cell lymphoma." Blood **107**(3): 1174-7.

Hoque, M. O., S. Begum, et al. (2004). "Quantitative detection of promoter hypermethylation of multiple genes in the tumor, urine, and serum DNA of patients with renal cancer." Cancer Res **64**(15): 5511-7.

Howard, J. H., A. Frolov, et al. (2009). "Epigenetic downregulation of the DNA repair gene MED1/MBD4 in colorectal and ovarian cancer." Cancer Biol Ther **8**(1): 94-100.

Huang, Y., A. de la Chapelle, et al. (2003). "Hypermethylation, but not LOH, is associated with the low expression of MT1G and CRABP1 in papillary thyroid carcinoma." International Journal of Cancer **104**(6): 735-744.

Ibanez de Caceres, I., E. Dulaimi, et al. (2006). "Identification of novel target genes by an epigenetic reactivation screen of renal cancer." Cancer Res **66**(10): 5021-8.

Ibragimova, I., I. Ibanez de Caceres, et al. (2010). "Global reactivation of epigenetically silenced genes in prostate cancer." Cancer Prev Res (Phila) **3**(9): 1084-92.

Izawa, J. I., M. Moussa, et al. (1998). "Metallothionein expression in renal cancer." Urology **52**(5): 767-72.

James R. Marthick, A. F. H. a. J. L. D. (2011). Prostate Cancer - From Bench to Bedside. Rijeka, Croatia, InTech.

Jomova, K. and M. Valko (2011). "Advances in metal-induced oxidative stress and human disease." Toxicology **283**(2-3): 65-87.

Kelly, T. K., D. D. De Carvalho, et al. (2010). "Epigenetic modifications as therapeutic targets." Nature biotechnology **28**(10): 1069-1078.

Kierszenbaum, A. L. (2002). "Genomic imprinting and epigenetic reprogramming: Unearthing the garden of forking paths." Molecular Reproduction and Development **63**(3): 269-272.

Kojima, I., T. Tanaka, et al. (2009). "Metallothionein is upregulated by hypoxia and stabilizes hypoxia-inducible factor in the kidney." Kidney Int **75**(3): 268-77.

Krizkova, S., M. Ryvolova, et al. (2012). "Metallothioneins and zinc in cancer diagnosis and therapy." Drug Metabolism Reviews **44**(4): 287-301.

Kuang, S. Q., H. Bai, et al. (2010). "Aberrant DNA methylation and epigenetic inactivation of Eph receptor tyrosine kinases and ephrin ligands in acute lymphoblastic leukemia." Blood **115**(12): 2412-9.

Laemmli, U. K. (1970). "Cleavage of structural proteins during the assembly of the head of bacteriophage T4." Nature **227**(5259): 680-5.

Laird, P. W. (2003). "The power and the promise of DNA methylation markers." Nat Rev Cancer **3**(4): 253-66.

Latif, F., K. Tory, et al. (1993). "Identification of the von Hippel-Lindau disease tumor suppressor gene." Science **260**(5112): 1317-20.

Lawrence, M. S., P. Stojanov, et al. (2014). "Discovery and saturation analysis of cancer genes across 21 tumour types." Nature **505**(7484): 495-501.

Lee, E. Y. and W. J. Muller (2010). "Oncogenes and tumor suppressor genes." Cold Spring Harb Perspect Biol **2**(10): a003236.
Lee, M. G., J. S. Huh, et al. (2006). "Promoter CpG hypermethylation and downregulation of XAF1 expression in human urogenital malignancies: implication for attenuated p53 response to apoptotic stresses." Oncogene **25**(42): 5807-5822.
Linehan, W. M., G. Bratslavsky, et al. (2010). "Molecular diagnosis and therapy of kidney cancer." Annu Rev Med **61**: 329-43.
Linehan, W. M., R. Srinivasan, et al. (2010). "The genetic basis of kidney cancer: a metabolic disease." Nat Rev Urol **7**(5): 277-85.
Lipworth, L., R. E. Tarone, et al. (2006). "The epidemiology of renal cell carcinoma." J Urol **176**(6 Pt 1): 2353-8.
Livak, K. J. and T. D. Schmittgen (2001). "Analysis of Relative Gene Expression Data Using Real-Time Quantitative PCR and the 2−ΔΔCT Method." Methods **25**(4): 402-408.
Lynch, C. F., M. M. West, et al. (2007). Cancers of the Kidney and Renal Pelvic. Cancer Survival Among Adults: US SEER Program, 1988-2001, Patient and Tumor Characteristics. SEER Program. M. J. Horner, J. L. Young and G. E. e. a. Keel, NIH Pub. No. 07-6215. Bethesda, MD: National Cancer Institute**:** 193–202.
Maher, E. R. (2013). "Genomics and epigenomics of renal cell carcinoma." Semin Cancer Biol **23**(1): 10-7.
Mathew, A., S. S. Devesa, et al. (2002). "Global increases in kidney cancer incidence, 1973-1992." Eur J Cancer Prev **11**(2): 171-8.
Mishra, A. and M. Verma (2010). "Cancer Biomarkers: Are We Ready for the Prime Time?" Cancers **2**(1): 190-208.
Momparler, R. L. (2003). "Cancer epigenetics." Oncogene **22**(42): 6479-83.
Morris, M. R., L. B. Hesson, et al. (2003). "Multigene methylation analysis of Wilms' tumour and adult renal cell carcinoma." Oncogene **22**(43): 6794-801.
Morris, M. R. and E. R. Maher (2010). "Epigenetics of renal cell carcinoma: the path towards new diagnostics and therapeutics." Genome Med **2**(9): 59.
Morris, M. R., E. Maina, et al. (2004). "Molecular genetic analysis of FIH-1, FH, and SDHB candidate tumour suppressor genes in renal cell carcinoma." J Clin Pathol **57**(7): 706-11.
Morris, M. R., C. J. Ricketts, et al. (2011). "Genome-wide methylation analysis identifies epigenetically inactivated candidate tumour suppressor genes in renal cell carcinoma." Oncogene **30**(12): 1390-401.
Mosmann, T. (1983). "Rapid colorimetric assay for cellular growth and survival: application to proliferation and cytotoxicity assays." J Immunol Methods **65**(1-2): 55-63.
Mund, C. and F. Lyko (2010). "Epigenetic cancer therapy: Proof of concept and remaining challenges." Bioessays **32**(11): 949-57.
Nardinocchi, L., V. Pantisano, et al. (2010). "Zinc downregulates HIF-1alpha and inhibits its activity in tumor cells in vitro and in vivo." PLoS One **5**(12): e15048.
Nath, K. A. (2005). "Provenance of the protective property of p21." Am J Physiol Renal Physiol **289**(3): F512-3.
Nguyen, A., Z. Jing, et al. (2000). "In vivo gene expression profile analysis of metallothionein in renal cell carcinoma." Cancer Lett **160**(2): 133-40.
Noren, N. K., G. Foos, et al. (2006). "The EphB4 receptor suppresses breast cancer cell tumorigenicity through an Abl-Crk pathway." Nat Cell Biol **8**(8): 815-825.
Oosterwijk, E., W. K. Rathmell, et al. (2011). "Basic research in kidney cancer." Eur Urol **60**(4): 622-33.
Palmiter, R. D. (1998). "The elusive function of metallothioneins." Proceedings of the National Academy of Sciences **95**(15): 8428-8430.
Pan, Y., J. Huang, et al. (2013). "Metallothionein 2A inhibits NF-kappaB pathway activation and predicts clinical outcome segregated with TNM stage in gastric cancer patients following radical resection." J Transl Med **11**: 173.
Park, C. C., M. J. Bissell, et al. (2000). "The influence of the microenvironment on the malignant phenotype." Mol Med Today **6**(8): 324-9.

Patra, A., M. Deb, et al. (2011). "5-Aza-2'-deoxycytidine stress response and apoptosis in prostate cancer." Clin Epigenetics **2**(2): 339-48.
Pedersen, M. O., A. Larsen, et al. (2009). "The role of metallothionein in oncogenesis and cancer prognosis." Prog Histochem Cytochem **44**(1): 29-64.
Pfaffl, M. W. (2001). "A new mathematical model for relative quantification in real-time RT–PCR." Nucleic Acids Research **29**(9): e45.
Pischon, T., P. H. Lahmann, et al. (2006). "Body size and risk of renal cell carcinoma in the European Prospective Investigation into Cancer and Nutrition (EPIC)." Int J Cancer **118**(3): 728-38.
Portela, A. and M. Esteller (2010). "Epigenetic modifications and human disease." Nat Biotechnol **28**(10): 1057-68.
Poste, G. (2011). "Bring on the biomarkers." Nature **469**(7329): 156-7.
Rodriguez-Paredes, M. and M. Esteller (2011). "Cancer epigenetics reaches mainstream oncology." Nat Med **17**(3): 330-9.
Ruiz-Magana, M. J., J. M. Rodriguez-Vargas, et al. (2012). "The DNA methyltransferase inhibitors zebularine and decitabine induce mitochondria-mediated apoptosis and DNA damage in p53 mutant leukemic T cells." Int J Cancer **130**(5): 1195-207.
Ruttkay-Nedecky, B., L. Nejdl, et al. (2013). "The role of metallothionein in oxidative stress." Int J Mol Sci **14**(3): 6044-66.
Sato, M. and M. Kondoh (2002). "Recent studies on metallothionein: protection against toxicity of heavy metals and oxygen free radicals." Tohoku J Exp Med **196**(1): 9-22.
Sato, Y., T. Yoshizato, et al. (2013). "Integrated molecular analysis of clear-cell renal cell carcinoma." Nat Genet **45**(8): 860-7.
Scaffidi, P. and T. Misteli (2010). "Cancer epigenetics: from disruption of differentiation programs to the emergence of cancer stem cells." Cold Spring Harbor symposia on quantitative biology **75**: 251-8.
Srinivas, P. R., M. Verma, et al. (2002). "Proteomics for cancer biomarker discovery." Clin Chem **48**(8): 1160-9.
Stenram, U., B. Ohlsson, et al. (1999). "Immunohistochemical expression of metallothionein in resected hepatic primary tumors and colorectal carcinoma metastases." APMIS **107**(4): 420-4.
Stratton, M. R. (2011). "Exploring the genomes of cancer cells: progress and promise." Science **331**(6024): 1553-8.
Suzuki, J. S., N. Nishimura, et al. (2003). "Metallothionein deficiency enhances skin carcinogenesis induced by 7,12-dimethylbenz[a]anthracene and 12-O-tetradecanoylphorbol-13-acetate in metallothionein-null mice." Carcinogenesis **24**(6): 1123-32.
Suzuki, M., H. Shigematsu, et al. (2007). "Methylation and gene silencing of the Ras-related GTPase gene in lung and breast cancers." Ann Surg Oncol **14**(4): 1397-404.
Swanton, C. (2012). "Intratumor heterogeneity: evolution through space and time." Cancer Res **72**(19): 4875-82.
Takeshita, T., T. Arita, et al. (1997). "STAM, signal transducing adaptor molecule, is associated with Janus kinases and involved in signaling for cell growth and c-myc induction." Immunity **6**(4): 449-57.
Tost, J. (2010). "DNA Methylation: An Introduction to the Biology and the Disease-Associated Changes of a Promising Biomarker." Molecular Biotechnology **44**(1): 71-81.
Urakami, S., H. Shiina, et al. (2006). "Wnt Antagonist Family Genes as Biomarkers for Diagnosis, Staging, and Prognosis of Renal Cell Carcinoma Using Tumor and Serum DNA." Clinical Cancer Research **12**(23): 6989-6997.
Valastyan, S. and R. A. Weinberg (2011). "Tumor metastasis: molecular insights and evolving paradigms." Cell **147**(2): 275-92.
Varela, I., P. Tarpey, et al. (2011). "Exome sequencing identifies frequent mutation of the SWI/SNF complex gene PBRM1 in renal carcinoma." Nature **469**(7331): 539-42.
Vasudev, N. and R. Banks (2011). "Biomarkers of renal cancer." Biomarkers in Kidney Disease: 313 - 344.

Weikert, S., H. Boeing, et al. (2008). "Blood pressure and risk of renal cell carcinoma in the European prospective investigation into cancer and nutrition." Am J Epidemiol **167**(4): 438-46.

Yamashita, K., S. Upadhyay, et al. (2002). "Pharmacologic unmasking of epigenetically silenced tumor suppressor genes in esophageal squamous cell carcinoma." Cancer Cell **2**(6): 485-95.

Yeung, B. H., A. Y. Law, et al. (2012). "Evolution and roles of stanniocalcin." Mol Cell Endocrinol **349**(2): 272-80.

Yoo, C. B., J. C. Cheng, et al. (2004). "Zebularine: a new drug for epigenetic therapy." Biochem Soc Trans **32**(Pt 6): 910-2.

You, J. S. and P. A. Jones (2012). "Cancer genetics and epigenetics: two sides of the same coin?" Cancer Cell **22**(1): 9-20.

Zhang, L., W. Zhou, et al. (1997). "Gene Expression Profiles in Normal and Cancer Cells." Science **276**(5316): 1268-1272.

9 Curriculum vitae

For reasons of data protection,
the curriculum vitae is not included in the online version

10 Publications and abstracts

10.1 Publications

Alkamal I., Ikromov O., Tölle A., Florian F. T., Magheli A., Miller K., Krause H., Kempkensteffen C. An epigenetic screen unmasks metallothioneins as putative contributors to renal cell carcinogenesis. Urologia Internationalis. 2013 September. Submitted.

Ikromov O., Alkamal I., Magheli A., Ratert N., Sendeski M., Miller K., Krause H., Kempkensteffen C. Functional epigenetic analysis of prostate carcinoma - a role for seryl-tRNA synthetase (SARS)? Urologia Internationalis. 2013 August. Submitted.

10.2 Abstracts

Alkamal I., Ikromov O., Tölle A., Krause H. An epigenetic screen demasks metallothioneins as putative contributors to renal cell carcinogenesis. Der Urologe. January 2013;52(1):99-128. Abstract. 4. Symposium. Urologische Forschung Der Deutschen Gesellschaft für Urologie. Berlin 2012, Germany.

Jandrig, B., Ikromov, O., Alkamal, I., Wendler, J.J., Schostak, M., Miller, K., Krause, H. The role of PBRM1 as tumor suppressor gene in renal cell carcinomas. Der Urologe. January 2013;52(1):99-128. Abstract. 4. Symposium. Urologische Forschung Der Deutschen Gesellschaft für Urologie. Berlin 2012, Germany.

Ikromov O., Alkamal I., Magheli A., Kempkensteffen C., Miller K., Krause H. Pharmacological reactivation of epigenetically regulated genes in prostate cancer. Der Urologe. January 2013;52(1):99-128. Abstract. 4. Symposium. Urologische Forschung Der Deutschen Gesellschaft für Urologie. Berlin 2012, Germany.

Ikromov O., Jandrig B., Alkamal I., Schostak M., Miller K., Krause H. The SWI/SNF nucleosome-remodeling gene PBRM1-another tumor suppressor gene in renal cell carcinomas? Eur Urol Suppl. February 2012;11;e306. Abstract. 27th Annual EAU Congress. Paris, France.

11 Acknowledgement

I would like to thank everyone who helped me through my PhD work supporting me with all what was needed to achieve this work from discussions to advices and further cooperation.

My gratitude goes to Prof. Dr. rer. nat. habil. Matthias F. Melzig for accepting being my doctoral thesis advisor in the Freie Universität Berlin, and to Dr. med. Dr. phil. Klaus M. Beier for offering me the opportunity to carry out my research work at the Urologische Klinik (Direktor: Prof. Dr. med. Kurt Miller), Charite´- Universitätsmedizin Berlin. I would like to thank my supervisor Dr. Hans Krause for his scientific cooperation and guidance in my experimental designs, and for his supervison in every step leading my PhD work to the end.

I thank Frau U. Ungethüm and Herr R. Kuban for Affymetrix GeneChip® analyses and processing data sets at the Charité LFGC core facility. I also thank Frau Angelika Tölle for her contribution to the western blot experiment, and thank as well Frau Ines Baumert, Frau Waltraut Jekabsons, Frau Sabine Becker, Frau Dipl.-Ing. Bettina Ergün, Frau Silke Rabenhorst, and Frau Dr. rer. medic. Monika Jung for their excellent technical assistance and scientific advice.

Many gratitude to Prof. Dittgen for his mentorship, and a lot of gratitude goes to both Prof. Mouhi-Dien Jouma and to Prof. Abdul-Ghani Maa-Baared for their continueous support, advices, and constant concern throughout my research work.

Many thanks goes to my friends: Issam Abu-Taha, Ramzi Farra, Sarah Vella, Annika Fendler, Isabel Steiner, Odiljion Ikromov, Zofia Wot, Julia Liep, Khaled Youssef, Travis Miller, Abdul-Kader Sammakieh, Tarek Bekfani, and many many others.

All my thanks to my parents for their unlimited non stop support and for their continuous encouragement standing beside me in all difficulties leading my way to a successful life. Many greetings to my brothers and sister which I am lucky to have.

At the end lots of prayers for my country and many wishes for a better future.

12 Declaration of Academic Honesty

Hereby, I declare that I have carried out this thesis on my own, having used only the listed resources and tools.

_____

Berlin,